An S-methyltransferase that produces the climate-active gas dimethylsulfide is widespread across diverse marine bacteria

Yunhui Zhang[1,2†], Chuang Sun[1,3†], Zihua Guo[1†], Liyan Liu[1], Xiaotong Zhang[1], Kai Sun[1,3], Yanfen Zheng[4], Andrew J. Gates[3], Jonathan D Todd[1,3*] and Xiao-Hua Zhang[1,2*]

[1] Frontiers Science Center for Deep Ocean Multispheres and Earth System, College of Marine Life Sciences, and Institute of Evolution and Marine Biodiversity, Ocean University of China, Qingdao, China

[2] Laboratory for Marine Ecology and Environmental Science, Qingdao Marine Science and Technology Center, Qingdao, China

[3] School of Biological Sciences, University of East Anglia, Norwich Research Park, Norwich, United Kingdom.

[4] Marine Agriculture Research Center, Tobacco Research Institute of Chinese Academy of Agricultural Sciences, Qingdao, China

†These authors contributed equally to this work.

*Corresponding Author: Xiao-Hua Zhang, xhzhang@ouc.edu.cn； Jonathan D Todd, Jonathan.Todd@uea.ac.uk

Running title: Novel *S*-methyltransferase producing dimethylsulfide

Keywords: methanethiol, sulfide, dimethylsulfide, *S*-methyltransferase, bacteria

Abstract

Hydrogen sulfide (H_2S), methanethiol (MeSH) and dimethylsulfide (DMS) are abundant sulfur gases with roles in biogeochemical cycling, chemotaxis and/or climate regulation. Catabolism of the marine osmolyte dimethylsulfoniopropionate (DMSP) is a major source of DMS and MeSH, but both also result from *S*-methylation of H_2S via MddA, an H_2S and MeSH *S*-methyltransferase whose gene is abundant in soil but scarce in marine environments. Here we identify the *S*-adenosine methionine (SAM)-dependent MeSH and H_2S *S*-methyltransferase "MddH", which is widespread in diverse marine bacteria and some freshwater and soil bacteria. *mddH* is predicted in up to ~5% and ~15% of seawater and coastal sediment bacteria, respectively, which is considerably higher than *mddA*. Furthermore, marine *mddH* transcript levels are similar to those for the most abundant DMSP lyase gene *dddP*. This study implies that the importance of H_2S and MeSH *S*-methylation pathways in marine environments is significantly underestimated.

Introduction

Dimethylsulfide (DMS) is the largest natural sulfur source transferred from Earth's oceans to the atmosphere (~13-37 Tg annually)[1,2], and its oxidation products can act as cloud condensation nuclei that potentially impact the climate[3]. DMS also plays important roles in microbial metabolism, global sulfur cycling[4] and chemotaxis[5]. Dimethylsulfoniopropionate (DMSP) is thought to be the major bio-source of DMS via microbial DMSP lyase enzymes[6] (Fig. 1a). However, there are other aerobic and anaerobic DMSP-independent DMS production pathways, such as sulfide (H_2S) and methanethiol (MeSH) *S*-methylation[7–9] (Fig. 1a). Microorganisms can produce MeSH from methionine (Met) cleavage[10], H_2S *S*-methylation[11], DMS degradation[12] and DMSP demethylation[13] (Fig. 1a), which accounts for >70% of marine DMSP catabolism[14]. Indeed, the ability to produce MeSH from Met (via MegL) and the DMSP demethylation intermediate methylmercaptopropionate (MMPA, via DmdBCD) is widespread in bacteria[15]. H_2S is also abundant in diverse environments, present at mM levels in e.g., sediment and hydrothermal environments[16,17].

MddA is a microbial SAM-dependent *S*-methyltransferase that *S*-methylates MeSH[8] and H_2S[9] to yield DMS (Fig. 1a), which can function to detoxify of H_2S and MeSH[9]. Though abundant in soil (relative abundance, RA, 5–76%) and surface saltmarsh sediment (RA 9.6%) bacteria, *mddA* is less common in seawater bacteria (RA ≤ 0.5%)[8,18,19]. However, Carrión et al. identified marine bacteria with MeSH-dependent DMS production (Mdd) activity that lacked *mddA*, implying the existence of unidentified Mdd enzymes[19]. Recently, thiol methyltransferases, termed TMT1A and

TMT1B, capable of methylating H_2S were identified in humans, other mammals and fish[20,21], but as yet no more in bacteria. Here we identify a bacterial thiol methyltransferase that allowed reevaluation of the importance of Mdd pathways as sources of DMS in marine settings.

Results

Methanethiol-dependent DMS production by Halomonas species

Halomonas alimentaria EF61 (isolated from Mariana Trench seawater[22]) produced MeSH and DMS when grown with L-Met (Fig. 1b). EF61 did not produce DMSP, thus its DMS production was not due to DMSP cleavage despite this bacterium exhibiting DMSP cleavage with exogenous DMSP (Fig. 1c). EF61 produced 11.3±3.1 nmol DMS·mg total protein^{-1}·h^{-1} from MeSH (Fig. 1d). EF61 also produced MeSH and DMS from MMPA (Fig. 1e), the primary catabolite of the DMSP demethylase predicted to be in ~20% of marine bacteria[15], and from H_2S (Fig. 1f). DMS production from L-Met, MMPA, MeSH and H_2S was also observed in 3/5 other tested *Halomonas* strains (SCS19, H33-56 and RT37) from diverse marine environments (Fig. 1, Supplementary Table 1). In contrast, *H. alimentaria* H10-9-1 and *H. saccharevitans* H10-59 could not generate DMS from any of these sulfur compounds but could produce MeSH from L-Met, MMPA and H_2S (Fig. 1). This data implied that H10-9-1 and H10-59 lacked or did not express key MeSH *S*-methyltransferase enzyme/s that were active in the four other *Halomonas* strains.

MddH, a H_2S and MeSH S-*methyltransferase in Halomonas*

The genomes of all six *Halomonas* isolates contained *megL* encoding Met γ-lyase, consistent with their ability to liberate MeSH from L-Met (Fig. 1a and 1b). They contained *dmdBC* and *acuH*, encoding enzymes that catabolize MMPA and release MeSH[15], consistent with their observed MMPA-dependent MeSH production phenotype (Fig. 1a and 1e). Like *Halominas* HTNK1[23], the strains contained the DMSP lyase gene *dddD* and generated DMS from exogenously added DMSP, and acetyl CoA, likely produced intracellularly[24] (Fig. 1a and 1c). None of the isolates contained *mddA*, encoding the only known microbial H_2S and MeSH *S*-methyltransferase, or proteins with > 63% coverage and > 34% amino acid identity to the human thiol *S*-methyltransferases TMT1A and TMT1B, indicating that the four *Halomonas* isolates with Mdd activity likely contained an unidentified Mdd enzyme.

There were 84 genes unique to the four *Halomonas* strains with Mdd activity compared to the two lacking this phenotype, and only one encoded a candidate methyltransferase. This gene, termed *mddH*, was associated to multicopper oxidase genes and those predicted to be involved in metal transport and resistance, with no obvious link to sulfur metabolism (Supplementary Fig. 1). MddH shared no protein sequence identity with MddA. Instead, it encoded a ubiquinone methyltransferase UbiE family protein (COG2226) with only 37% amino acid identity to *E. coli* UbiE, a SAM-dependent methyltransferase involved in menaquinone synthesis[25]. Notably, all six *Halomonas* strains contained a different UbiE homologue, with 74-75 % protein identity to *E. coli* UbiE. EF61 MeSH *S*-methylation activity was cytosolic (2.46±0.3 nmol DMS·mg total

protein$^{-1}\cdot h^{-1}$) and not membranous, consistent with the EF61 MddH protein lacking a signal peptide. This differs from MddA which has 4-6 membrane spanning helices and whose activity is enriched in *Pseudomonas deceptionensis* membrane fractions[8]. Indeed, MeSH *S*-methylation activity was detected in the cytosolic (2.46±0.3 nmol DMS·mg total protein$^{-1}\cdot h^{-1}$) but not in membrane fractions of *H. alimentaria* EF61.

The MddH protein shared 31/50% and 34/53% amino acid sequence identity/similarity to the human thiol *S*-methyltransferases TMT1A and TMT1B, respectively, and their AlphaFold[26] predicted structures were similar, particularly in their central and C-terminal regions, containing the conserved central GxGxG binding motif[21] for SAM binding (Supplementary Fig. 2a). The predicted MddH structure was comparatively more compact than for TMT1A and TMT1B, lacked an extended N-terminal 'hooked' helical region and a conserved aspartate residue at position 98 previously implicated in SAM binding[21], which was a glutamate at position 63 in MddH (Supplementary Fig. 2b). These observations support the hypothesis that MddH was a thiol *S*-methyltransferase like TMT1A and TMT1B.

E. coli cell extracts containing EF61 MddH protein showed *in-vitro* SAM-dependent Mdd activity (46.4±4.0 nmol DMS·mg total protein$^{-1}\cdot h^{-1}$) and H_2S-dependent MeSH (14.4±1.5 nmol·mg total protein$^{-1}\cdot h^{-1}$) and DMS (10.3±0.2 nmol·mg total protein$^{-1}\cdot h^{-1}$) production (Table 1). Furthermore, an EF61 Δ*mddH* mutant (Supplementary Fig. 3a) overproduced MeSH when grown with L-Met or H_2S compared to the wild type strain and completely lacked Mdd activity (Supplementary Fig. 3b and 3c). These mutant phenotypes were restored to wild type levels by cloned *mddH*, consistent with MddH

being the *Halomonas* spp. SAM-dependent MeSH *S*-methyltransferase enzyme. These data and those in Fig. 1 indicated that there were also MddH-independent pathways converting H_2S to MeSH in the tested *Halomonas* strains studied here, potentially through L-cysteine and L-Met as intermediates[27,28].

Importantly, when incubated in sterilized coastal seawater with 4 nM H_2S or MeSH, EF61 and not the Δ*mddH* mutant showed significant DMS production (Supplementary Table 2) compared to the seawater control. The H_2S or MeSH levels used were physiologically relevant for seawater and sediment samples[29,30], implying that MddH yields DMS in marine environments.

MddH is widespread in diverse bacteria

Proteins with > 45% amino acid identity to MddH were identified in diverse bacterial taxa, mainly *Gammaproteobacteria* and *Alphaproteobacteria*, but also some *Betaproteobacteria*, *Deltaproteobacteria, Acidobacteria*, and *Bacteroidetes* (Fig. 2). When cloned, candidate *mddH* genes from marine and soil bacteria, but not *Vibrio ubiE* (negative control) conferred H_2S and Mdd *S*-methylation activity to *E. coli* (Table 1). This included ^{Ml}MddH from *Marinobacter litoralis* Sw-45, characterized below, that shared 60.3% amino acid identity to EF61 MddH. The diverse natural host bacteria containing *mddH* genes also had H_2S and MeSH *S*-methylation activity (Supplementary Fig. 4). We predict that the candidate MddH enzymes in Fig. 2, which are distinct from the UbiE outgroup, constitute the "MddH" family of H_2S and MeSH *S*-methyltransferase enzymes. Several SAM-dependent methyltransferases were

structurally similar to MddH (predicted by AlphaFold), but these had < 21% amino acid identity to MddH, broad substrate specificity where characterized (Supplementary Table 3), and require examination to determine their activity on H_2S/MeSH.

Interestingly, *M. litoralis* Sw-45 *mddH* was adjacent to the *cydABCD* operon encoding a cytochrome *bd* oxidase complex (CydAB) and cysteine transporter (CydDC) involved in the regulation of intracellular cysteine and redox levels and H_2S production[31,32]. However, *mddH* was not associated to any genes obviously linked to the H_2S or MeSH generation in other bacteria (Supplementary Fig. 1).

mddH and *mddA* were found in distinct but similarly diverse host bacteria. The *mddA* gene was mostly found in actinobacterial, alphaproteobacterial *Rhizobiales* and except *Pseudomonas* was far less common in gammaproteobacteria than *mddH*[8]. The key difference between bacteria containing *mddA* and *mddH* was not in their host taxonomy, but more prominently in the environments they inhabit. Most bacteria with *mddA* were isolated from terrestrial soil or freshwater and not marine environments[8]. In contrast, *mddH* was predominantly in diverse bacteria from marine seawater or sediment such as *Halomonas*, *Marinobacter*, *Novosphingobium* and *Erythrobacter* (Fig. 2). *mddH* was also found but far less frequent in bacteria from soil, lake, spring, and other sources like wastewater plants, compost, fruits or animals (Fig. 2).

Characterization of the MddH enzyme

The purified *M. litoralis* Sw-45 MddH enzyme (Fig. 3a) showed SAM-dependent *S*-methylation of H_2S and MeSH, producing both MeSH and slightly lower amounts of

DMS from H_2S (Fig. 3b). ^{Ml}MddH had an optimal pH of ~9.0 (Supplementary Fig. 5a) and temperature of 45 °C (Supplementary Fig. 5b) for MeSH and H_2S, and showed high activities at ~pH 8 and between 10-20 °C, physiologically relevant seawater pH and temperature values, respectively (Supplementary Fig. 5). ^{Ml}MddH had K_m and k_{cat} values of 0.23 mM and 0.08 $s^{-1}$for MeSH, respectively, and 0.07 mM and 0.06 s^{-1} for the SAM co-substrate, respectively. The K_m of ^{Ml}MddH for H_2S (0.22 mM) was similar to that for MeSH (0.23 mM), while the k_{cat} value of 0.16 s^{-1} measured for H_2S was about 2-fold higher than that for MeSH (Fig.3e and 3f). Overall, ^{Ml}MddH was ~2-fold more efficient using H_2S (k_{cat}/K_m ~727 $M^{-1}\cdot s^{-1}$) over MeSH (k_{cat}/K_m ~347 $M^{-1}\cdot s^{-1}$) as substrate. ^{Ml}MddH turnover rates for H_2S (0.16 s^{-1}) and MeSH (0.08 s^{-1}) were consistent with enzymes involved in secondary metabolism[33] and the SAM-dependent *S*-methyltransferase MddA with MeSH (~0.09 s^{-1}) and H_2S (~0.01 s^{-1})[9]. Compared to MddA, the specificity constants for ^{Ml}MddH with H_2S and MeSH were substantially higher by around an order of magnitude indicating higher catalytic efficiency. The modestly lower k_{cat}/K_m values observed for ^{Ml}MddH relative to the lower limit expected for most enzymes[33] may be due to the reactive nature of these gaseous substrates and/or substrate diffusion limitation in assays. ^{Ml}MddH showed no *S*-methylation activity towards most other tested sulfur compounds including glutathione (GSH), cysteine (L-Cys), coenzyme A (CoA), 2-mercaptoethanesulfonate (Coenzyme M) or the DMSP synthesis intermediates L-Met and 4-methylthio-2-hydroxybutyrate (MTHB) (Fig 3c). However, *S*-adenosyl homocysteine was formed from SAM when ^{Ml}MddH was incubated with ethanethiol and 1-propanethiol at levels ~23 and ~40 % less,

respectively, compared to MeSH (Supplementary Fig. 5e). This is consistent with MddH being able to *S*-methylate other short chain low molecular weight alkyl thiols. The purified ^{Ml}MddH protein contained only up to 0.15 Zn and 0.038 Ca metals per protein and addition of mM levels of the metal chelator EDTA only slightly reduced its activity (Fig. 3d). Furthermore, MddH activity was not enhanced by the addition of various metals and was even reduced by mM levels of Mn^{2+}, Zn^{2+} and Co^{2+} (Supplementary Fig. 5c and 5d). Thus, despite *Halomonas mddH* being linked to candidate metal transporters and metalloenzymes (Supplementary Fig. 1), MddH does not likely require a metal co-factor for activity.

The role of MddH in bacteria

The wild type EF61, Δ*mddH* mutant and genetically complemented strains were assessed for their ability to grow with mM L-Met, H_2S, MeSH, cysteine, H_2O_2, cobalt or zinc levels. These compounds and metals can be cytotoxic if allowed to accumulate, cause oxidative stress [31,32,34] and/or were associated to the action of gene products situated near to *mddH* in microbial genomes (Supplementary Fig. 1). With the exception of MeSH, none of these compounds or metals significantly affected the growth or yield of the Δ*mddH* compared to the wild type strain (Supplementary Fig. 6). In contrast, despite having a similar initial growth rate to the wild type and complemented strains, the Δ*mddH* mutant had significantly reduced final biomass when grown with 2 mM MeSH compared to the wild type and complemented strains (Supplementary Fig. 6). Furthermore, *mddH* transcription was significantly 2.5-fold upregulated by growth with

MeSH but not L-Met or H_2S (Supplementary Fig. 6e). This data is consistent with MddH having a role to detoxify MeSH when it reaches high environmental levels, through generation of non-toxic DMS, as was recently shown for MddA[9]. Although MeSH is potentially abundant in Earth's oceans due to prominence of DMSP demethylation, it is rarely likely to reach mM levels[35]. Thus, if MddH does have a role in MeSH detoxification, it is likely minor under physiologically relevant marine conditions. Alternatively, we hypothesize there were other detoxification strategies for the MeSH and/or the other tested stress-inducing molecules in EF61 that compensate for the loss of MddH in the EF61/Δ*mddH* mutant. This hypothesis was supported by the MddH-independent *S*-methylation of H_2S observed with all *Halomonas* strains tested here (Fig. 1).

MddH is abundant in marine environments

mddH was found in 242 out of 243 *Tara* Oceans samples in the OM-RCG marine metagenome database[36], comprising 68 sampling locations in epipelagic and mesopelagic waters across the globe. In the 178 prokaryote-enriched samples (>0.22 μm size-fractionated), the percentage of *mddH* normalized by cell numbers ranged between 0.09%-5.2% (with an average of 2.19 ± 0.93%) (Fig. 4, Supplementary Table 4). Marine samples with abundant *mddH*-containing bacteria (>4%) were from the South/North Atlantic Ocean, South/North Pacific Ocean, Indian Ocean and Mediterranean Sea. The relative abundance of *mddH* in surface water (SRF, median: 2.26%) and the deep chlorophyll maximum layers (DCM, median: 2.21%) were similar,

but were significantly higher than in the mesopelagic zone (MES, median: 1.60%) (Kruskal-Wallis test, Chi square=16.0, df=2, $p<0.05$) (Supplementary Fig. 7). Surprisingly, many copies of *mddH* were also identified in virus enriched samples (<0.22 μm) (5.79×10^{-8}-4.06×10^{-5} per mapped read). Indeed, 32 distinct MddH homologues were identified from marine viruses in Tara Oceans Viromes[37] data. Many of these were highly homologous to bacterial *mddH* genes (Supplementary Table 5, Supplementary Fig. 8), supporting the hypothesis of *mddH* horizontal gene transfer between viruses and bacteria. In contrast, *mddA* was detected in far less *Tara* Oceans (190 of the 243) and marine prokaryote-enriched samples (169 of 178) than *mddH*. *mddA* was significantly less abundant than *mddH* in these samples (~50-fold lower, Mann-Whitney test, $p<0.05$) with on average only 0.04±0.07% of bacteria predicted to contain *mddA* (Supplementary Table 4). Additionally, unlike *mddH*, the percentage of bacteria with *mddA* was highest in the MES samples (Kruskal-Wallis test, Chi square=34.8, df=2, $p<0.05$). The 216 *mddH* sequences retrieved from *Tara* Oceans metagenomes were all from *Proteobacteria* (73.1% *Gammaproteobacteria*, 12.0% *Alphaproteobacteria*, 0.5% *Betaproteobacteria* and 14.4% others) (Fig. 4b). In contrast, the 25 *mddA* sequences were distributed in more diverse bacterial taxa, including *Bacteroidetes*, *Cyanobacteria*, *Planctomycetes* and *Alpha-*, *Gamma-* and *Epsilon-proteobacteria* (Fig. 4b).

mddH and *mddA* transcripts were found in 186 and 63, respectively, of the 187 metatranscriptomes in the OM-RGCv2 database[38] (Fig. 4c). Consistent with their gene abundance, the abundance of *mddH* transcripts (2.80×10^{-7}- 5.33×10^{-5} per mapped read)

was far higher than for *mddA* (4.84×10^{-9}- 8.03×10^{-7} per mapped read). These data are consistent with MddH being an important enzyme in Earth's oceans and marine H_2S and MeSH *S*-methylation which is more significant than previously predicted[8].

In contrast, the most abundant DMSP lyase gene *dddP* was predicted to be in 12.4% ± 6.7% (0.4%-29.3%) of bacteria in *Tara* Oceans metagenomes, which was ~ 5-fold more than those with MddH (Supplementary Table 4). *dddP* transcript levels (2.78×10^{-7}-9.98×10^{-5} per mapped read) were also slightly higher than those of *mddH* (1.86×10^{-7}-5.32×10^{-5} per mapped read). These data imply that the Mdd pathway is likely a less important source of DMS than DMSP-dependent DMS production in marine systems.

As much as ~15% of bacteria (0.88 % - 14.74 %, normalized by cell number) in surface sediments from the Bohai and Yellow Sea near China[39] were predicted to contain *mddH* (Fig. 4d). Indeed, *mddH* was far more abundant than *mddA* (predicted in 0.39-3.34% of bacteria) in most samples. These 'omics data again suggest that bacteria with *mddH* and *mddA* are generally more abundant in sediment than aquatic marine samples, and that *mddH* is the dominant gene in these marine settings (Fig. 4d). Sediment *mddH* genes were mainly gammaproteobacterial but were also in *Acidobacteria* and some sulfate reducing *Deltaproteobacteria*, whereas *mddA* was found in more diverse phyla including *Ignavibacteriae*, *Nitrospirae*, *Planctomycetes* and *Bacteroidetes* (Fig. 4e). These sediment environments likely contain higher physiological levels of L-Met, MeSH and, more prominently, H_2S (that can be present at mM levels), than seawater environments[22,39] . However, the genetic potential to cleave DMSP was still higher in these sediments, with 10.0%-29.5% of bacteria predicted to contain *dddP.* Once again,

this implies DMSP cleavage as the likely dominant DMS-producing pathway. Nevertheless, considering the large number of bacteria in marine sediment[40] and the often high substrate availability[22,39], H_2S- and MeSH-dependent DMS production pathways are likely significant sources of DMS in marine sediment environments.

Given Carrión et al.[8] predicted that 5–76% of soil bacteria contained *mddA* from metagenomic analysis, we also examined the abundance of *mddH* in these soil metagenomes (Supplementary Table 6)[8]. No reliable *mddH* sequence was identified in these soil metagenomes possibly due to their sequence depth. Thus, we also investigated the abundance of *mddA* and *mddH* in larger metagenome datasets from rhizosphere soil samples of different plants (*Glycine soja*, *Sesbania cannabina* and *Sorghum bicolor*)[41]. Only 0.1%-1.67% of bacteria in these soil samples were predicted to contain *mddH*, whereas *mddA* was far more abundant (8.74%-13.11%) (Supplementary Fig. 9). These data are consistent with MddA being the major H_2S and MeSH *S*-methylation enzyme in terrestrial soils, whilst MddH likely dominates in marine settings.

Discussion

MddH is a SAM-dependent H_2S and MeSH *S*-methyltransferase, which is phylogenetically distinct to bacterial MddA and human TMT1A and TMT1B (Supplementary Fig. 10). Importantly, MddH was in up to ~5% and ~15% of bacteria in seawater and coastal sediments, which equates to 2.6×10^4 and 2.85×10^8 bacteria per g/ml[22,42], respectively containing *mddH* and the capacity to *S*-methylate H_2S and MeSH

300 to yield DMS. These findings challenged the view that Mdd processes were only likely
301 significant in soil bacteria[8,9], emphasizing a potentially important and unexpected role
302 for this pathway in global marine sulfur cycling.
303 Notably, L-Met is potentially toxic to cells if allowed to accumulate[43] and is a substrate
304 for both DMSP biosynthesis and Mdd via the MegL enzyme which liberates MeSH and
305 is common to most bacteria. Thus, both these pathways potentially alleviate the cellular
306 toxicity of excess cellular L-Met since DMSP and DMS are non-toxic molecules. Far
307 less marine bacteria contain the dominant DMSP biosynthesis gene *dsyB* (0.5% of
308 bacteria[44]) than *megL* and *mddH*, implying that MddH may have a more prominent role
309 in the management of free L-Met in marine bacteria. H_2S and MeSH are also cytotoxic,
310 which animals and plants detoxify by enzymatic *S*-methylation, in many cases, to
311 DMS[45,46]. Whilst the data presented here supported the role of MddH in the
312 detoxification of MeSH, its role in detoxification excess H_2S was not supported, since
313 the *Halomonas mddH*$^-$ mutant showed no growth or yield impairment compared to the
314 wildtype in the presence of this toxic molecule. There were likely other H_2S *S*-
315 methylation pathways which may have compensated for the loss of *mddH*. Nevertheless,
316 bacterial DMSP biosynthesis genes and *mddH* were generally more abundant in marine
317 sediments than waters, as are L-Met, MeSH and H_2S, indicating that diverse sediments
318 might be environments with high levels of not only DMSP but also DMS produced
319 through the MeSH and H_2S *S*-methylation and DMSP cleavage pathways.
320 Considering the enormous scale of DMSP production[47] and the high abundance of
321 diverse microbial *ddd* genes[6] in marine settings, DMSP cleavage is still likely the

dominant DMS-producing pathway in marine aquatic environments. However, it should not be forgotten that DMSP demethylation which produces MeSH is thought to account for 70% of marine DMSP catabolism[48] and that H_2S can reach mM levels in marine sediments[16,17], indicating the presence of considerable amounts of the MeSH and H_2S substrates for MddA and MddH in marine settings. Compared to DMS, there are few measurements of MeSH and H_2S from aerobic marine environments, but they are generally thought to be far less abundant than DMS[49], which may be due in part to an active marine MeSH and H_2S *S*-methylation pathway, particularly via MddH. Further studies evaluating MeSH and H_2S *S*-methylation and its flux in diverse marine settings are required to establish its impact on global DMS production and sulfur cycling, but this study implies that these methylation reactions are far more important in marine environments than previously predicted.

Methods

Bacterial strains and culturing

Detailed information of the strains used in this study are listed in Supplementary Table 1. *Escherichia coli* strains were grown on LB media overnight at 37 ℃. *Halomonas* strains and other marine bacterial isolates were routinely grown on Marine Agar (MA) medium (per liter seawater: 1 g yeast extract, 5 g peptone, 0.01 g ferric phosphate, 2 g agar, pH 7.6) for 24 h at 28 ℃. These isolates were also cultivated in marine basal medium (MBM) minimal medium (salinity 35 PSU)[50] supplemented with a mixed carbon source (10 mM from a 1 M stock of 200 mM succinate, glucose, pyruvate,

sucrose, and glycerol).

Quantification of DMS and MeSH production

To measure DMS and MeSH production by *Halomonas* strains, colonies from fresh agar plates were inoculated into 200 μL MBM medium supplemented with or without L-Met and MMPA (0.5 mM final concentration) in 2 mL sealed glass vials, and incubated at 28 ℃, 170 rpm for 24 h. The headspace MeSH and DMS was monitored by gas chromatography (GC) with a flame photometric detector (Agilent 7890B GC fitted with a 7693A autosampler) and an HP-INNOWax 30 m× 0.320 mm capillary column (Agilent Technologies J&W Scientific). DMS and MeSH calibration curves were produced as described by Curson et al.[8]. The detection limits for DMS and MeSH were 0.2 and 5 nmol, respectively. Cellular protein content was estimated by Bradford assays (BioRad, Hemel Hempstead, UK). Rates of MeSH and DMS production were expressed as nmol h^{-1} per mg total protein. Experiments were carried out in three biological replicates. To measure DMS production from MeSH, *Halomonas* strains were cultured in MBM supplemented with 0.5 mM MeSH as described above. To measure MeSH and DMS production from H_2S, *Halomonas* strains were cultured in Marine Broth (MB) medium (per liter seawater: 1 g yeast extract, 5 g peptone, pH 7.6) supplemented with 0.5 mM H_2S, since H_2S was reactive with Fe(III)EDTA in the MBM. To measure DMSP production, *Halomonas* strains were cultured in MBM with L-Met (0.5 mM) in 1.5 ml Eppendorf tubes at 28 ℃, 170 rpm for 24 h, then 200 μl of NaOH (10 M) was added 200 μl of cultures, immediately sealed and mixed in 2 mL glass vials to chemically cleave the DMSP and yield DMS. Vials were incubated in the dark

overnight and the DMS derived from DMSP was measured by GC, as above. To measure DMSP catabolism, strains were cultured in MBM with DMSP (0.5 mM) in 2 mL sealed glass vials at 28 ℃, 170 rpm for 24 h. The resulting DMS was measured and quantified as described above.

Genome sequencing and comparative genomic analysis

Genomic DNA from six *Halomonas* strains was extracted following the phenol-chloroform-isoamylic alcohol extraction protocol. Genomic DNA sequencing and quality control was performed by the Beijing Genomics Institute (BGI; Shenzhen, China) using Illumina Hiseq 4,000 with a 270 bp pair-end library and PacBio with a 20 kb library. The PacBio reads and Illumina reads were assembled by Unicycle (v0.4.8). Annotation of these genomes were conducted by Prokka[51] (for comparative genomic analysis) and the RASTtk online service[52] with default settings. General features of six *Halomonas* genomes are listed in Supplementary Table 7. Ratified protein sequences of MddA, MegL and other enzymes involved in DMS cycling described by Song et al.[39] were used as query sequences to perform BLASTP against six *Halomonas* genomes. The program GET_HOMOLOGUES v3.0.3[53], with three clustering algorithms, *i.e.* bidirectional best hit (BDBH), COGtriangles and OrthoMCL, was used for clustering orthologous genes and identifying core- and pan-genomes under default parameter values. Unique genes belonging to DMS-producing *Halomonas* strains compared with non-DMS-producing isolates were extracted.

Construction in-frame deletion mutant of mddH

An in-frame deletion mutation of *mddH* (Δ*mddH*) was constructed in *H. alimentaria*

EF61 by double-crossover allelic exchange. The plasmids and primers used are listed in Supplementary Table 8 and 9. Briefly, the up- and downstream region of *mddH* was amplified by polymerase chain reaction (PCR) using primer pair *mddH*-UO/UI (product size: 660 bp) and *mddH*-DO/DI (product size: 766 bp), respectively. The two PCR products, above, were further used as templates in overlapping PCR using *mddH*-UO/DO to yield a final product of 1426 bp comprising the up- and downstream region of *mddH*. The resulting product was cloned into the pK18mobsacB suicide vector, and conjugated into *H. alimentaria* EF61 by triparental mating using the *E. coli* helper strain 803/pRK2013. Transconjugants with a single-crossover insertion in EF61 chromosome were obtained by screening on MA plates containing rifampicin (Rif) and kanamycin (Kan). Allelic exchange to delete a 483-bp core region within *mddH* (621 bp) was achieved by a second crossover event, which was selected on MA containing 20% (wt/vol) sucrose. The resultant mutant, EF61/Δ*mddH*, was selected by antibiotic sensitivity (Kan sensitive and Rif resistant) and confirmed by PCR assay followed by nucleotide sequence analysis (Supplementary Fig. 3a).

To complement the *mddH* mutation, the *mddH* gene containing its promoter region was amplified using primers *mddHcom*-F and *mddHcom*-R (Supplementary Table 9). The fragment was cloned into a low-copy plasmid pBBR1MCS-5, verified by sequencing, and transformed into the EF61/Δ*mddH* mutant by electroporation. The complemented strain (EF61/Δ*mddH/*pBBR1MCS-5-*mddH*) was selected as gentamycin-resistant transformants and the presence of the plasmid was confirmed by PCR analysis and sequencing. The EF61/Δ*mddH* mutant and complemented strain

EF61/Δ*mddH*/pBBR1MCS-5-*mddH* were grown on MA for 20 generations to ensure that they were stably maintained.

Seawater incubation experiments

H. alimentaria EF61 and the Δ*mddH* mutant were grown at 28 ℃, 170 rpm for 24 h in MB. Bacterial cells were harvested, washed three times and resuspended in sterilized seawater (collected from Qingdao coastal, October 2023). The resuspended cultures were 10-fold diluted into 2.5 mL sterilized seawater (with 4 nM MeSH or H_2S) in triplicate followed by incubation at 16 ℃ for further 24 h. The resulting DMS was quantified using a modified purge and trap method and GC[54].

Construction of the MddH phylogenetic tree

The *H. alimentaria* EF61 MddH protein sequence was used as a query sequence to perform a BLASTP search against the representative genome database in NCBI. Candidate MddH sequences with > 45 % identity and an E-value ≤ 1e−50 were chosen to construct MddH phylogenetic tree. All protein sequences were aligned by the Muscle method in MEGA 7.0.26 Package[55]. The Maximum-likelihood tree of MddH homologous was constructed by IQ-TREE (version 1.6.1) [56] under the LG+F+R6 model with 1,000 bootstrap replications. The UbiE Protein sequence from *Vibrio* sp. ZXX013 (ON685883), a strain with no Mdd activity, was used as an out-group. The resulting tree was visualized by iTol[57].

Prediction of MddH cell location in H. alimentaria EF61

The signal peptide and cell location of MddH was predicted by SignalP 6.0[58], Cello[59] and PortB[60]. The membrane and cytoplasmic proteins of *H. alimentaria* EF61 were

extracted using the Bacterial Membrane Protein/Cytoplasmic Protein Extraction Kit (Solarbio, Beijing, China) as the manufacturer's instructions, resulting in 24.3 $mg \cdot mL^{-1}$ membrane proteins and 23.3 $mg \cdot mL^{-1}$ cytoplasmic proteins. 600 μg membrane, cytoplasmic and total proteins were added in Tris-HCl (pH 9.0) with 1 mM MeSH and SAM, respectively, to a final volume of 150 μL and incubated at 37°C for 3 h. The DMS production was quantified as described above.

***Heterogenous expression of MddH* and homologous enzymes**

The *mddH* gene from *H. alimentaria* EF61 (621 bp, WP_013333065.1) was amplified by PCR using the primer set MddHPE-F/MddHPE-R (Supplementary Table 9) and cloned into the *E. coli* expression vector, pET-24a. The cloned gene was confirmed by sequencing at Sangon Biotech (Shanghai, China). The pET-24a construct containing *mddH* and empty vector controls were transformed into *E. coli* BL21 (DE3) cells and grown at 37 °C, 150 rpm in LB broth supplemented with Kan (100 μg mL^{-1}). At the mid-exponential growth phase, isopropylthio-*β*-galactoside (IPTG) was added at a final concentration of 0.1 mM, and the cells were then incubated at 28 °C, 150 rpm, for a further 3 h. The *E. coli* cells were then pelleted by centrifugation, resuspended in PBS buffer and sonicated as described by Carrion et al[8]. The supernatants were collected and cell pellets were resuspended. Triplicate 200 μL supernatants were incubated with 1 mM SAM and 1 mM MeSH (or 1 mM H_2S) for 2 h before quantifying the DMS (and MeSH) produced in the headspace and protein concentrations, as described above.

To define the functionality of the MddH protein family, candidate *mddH* genes from *Marinobacter litoralis* Sw-45 (WP_114333749.1), *Algiphilus aromaticivorans*

DG1253 (WP_043766208.1), *Pseudomonas pelagia* CL-AP6 (WP_022964284.1), *Hyphomonas adhaerens* MHS-3 (WP_035568920.1), *Pyruvatibacter mobilis* CGMCC_1.15125 (WP_160588566.1), *Novosphingobium colocasiae* KCTC 32255 (WP_189621457.1), *Erythrobacter ramosus* DSM 8510 (WP_160761066.1), *Ramlibacter aquaticus* LMG 30558 (WP_193782355.1) and *Caulobacter henricii* CB4 (WP_062144739.1) were obtained from NCBI (Supplementary Table 10), synthesized by Sangon Biotech (Shanghai, China) and cloned into pET-24a. The *ubiE* gene from *Vibrio* sp. ZXX013 with no Mdd activity, was also synthesized and cloned into pET-24a. Heterologous expression of these genes/proteins in *E. coli* and H_2S and MeSH *S*-methyltransferase assays were performed as described above.

Characterization of MddH enzyme properties

Heterologous expressed *M. litoralis* MddH protein was purified using NTA-Ni (Qiagen) according to the manufacturer's recommendations. The purified MddH was assessed by 12% sulfate-polyacrylamide gel electrophoresis (SDS-PAGE) and stored at −20°C with 25% glycerol. The enzymatic activity of MddH was determined in a standard reaction system containing 20 mM Tris-HCl buffer (pH 9.0), 1 mM SAM, 1 mM MeSH (or H_2S) and 0.27 μM of enzyme in a final volume of 150 μL. After incubation at 37 °C for 30 min, the reaction was terminated by adding 100 μL HCl (10%) and the production of DMS (and MeSH) was measured by GC as described above.

To determine the optimal catalysis temperature, the activity of MddH was measured at 4 to 65 °C at different intervals. The optimal pH values of MddH were measured between pH 4-10.6 with buffer systems described by He et al [61]. To analyze the effects

476 of metal ions on MddH activity, Mn^{2+}, Na^{+}, K^{+}, Zn^{2+}, Ca^{2+}, Mg^{2+} and Co^{2+} were added
477 at final concentrations of 0.1 and 1 mM. The effects of metal-chelator EDTA, and
478 protein denaturant SDS and urea were examined at final concentrations of 0.1 and 1
479 mM. Additionally, the metal concentrations (Zn, Pb, Mn, Mg, K, Fe, Cu, Co, Ca, Al
480 and Na) of the purified MddH were analyzed by Agilent 7500c inductively coupled
481 plasma mass spectrometry (ICP-MS). To test the substrate specificity, L-Met, MTHB,
482 glutathione (GSH), cysteine and CoA were added to a final concentration of 1 mM, and
483 the resulting *S*-adenosyl-L-homocysteine (SAH) from SAM was detected by High
484 performance liquid chromatography (HPLC) analyses[9].
485 K_m and k_{cat} values were determined by nonlinear analysis of kinetic data using 0.27 μM
486 MddH and 0-2 mM SAM (1 mM MeSH/H_2S), or 0-2 mM MeSH/H_2S (1 mM SAM) in
487 20 mM Tris-HCl (pH 9.0). The reaction mixture was incubated at 45°C for 30 min and
488 terminated by the addition of 100 μl 10% HCl before detection of DMS (and MeSH)
489 by GC. The MddH methyltransferase activity was reported as the amount of DMS
490 produced from MeSH, and by the sum amount of MeSH and twice DMS production
491 (since two methyl groups were transferred by MddH to produce DMS) with H_2S as
492 substrate. No background DMS production was detected with either SAM and MeSH
493 or SAM and H_2S in solution at 2 mM under these experimental conditions. Kinetic
494 parameters were calculated by non-linear regression fit directly to the Michaelis-
495 Menten equation using the Graphpad Prism8.
496 ***Growth of Halomonas strains under different conditions***
497 To compare the growth of *H. alimentaria* EF61, Δ*mddH* and the complemented strain,

498 overnight cultures of these strains were adjusted to the same absorbance at 590 nm and
499 inoculated (1:100) into MBM, and MBM supplemented with 2 mM of MeSH and H_2S.
500 The cultures were incubated at 28 ℃ and the absorbance at 595 nm was measured
501 hourly in 96-well plates. Each experiment was conducted in triplicates.
502 To investigate the direct influence of Co^{2+}, Zn^{2+}, H_2O_2 and cysteine on growth,
503 overnight cultures of *H. alimentaria* EF61, Δ*mddH* and the complemented strain were
504 adjusted to the same absorbance at 595 nm and inoculated (1:100) into 5 mL MBM
505 with Co^{2+}, Zn^{2+}, H_2O_2 or cysteine, respectively, added to a final concentration of 1 mM.
506 The cultures were incubated at 28 ℃, 170 rpm and the growth of each strain was
507 recorded after 24 h by measuring their absorbance at 595 nm. Each experiment was
508 conducted in triplicates.
509 ***RT-qPCR analysis***
510 *H. alimentaria* EF61 was cultured in Marine Broth (MB) at 28℃ until mid-exponential
511 phase. Cultures were harvested by centrifugation at 4,000 *g* for 5 min, rinsed and
512 resuspended in fresh MB. MeSH and H_2S were added to a final concentration of 1 mM
513 and the cells were incubated at 28℃ for 2h. The same volume of distilled water was
514 added in the control. Total RNA extraction was performed using E.Z.N.A Bacterial
515 RNAkit (Omega, China). Reverse transcription was performed using the TransScript
516 One-Step gDNA Removal and cDNA Synthesis SuperMix Transcript (TransGen,
517 China). RT-qPCR was performed on ABI 7500 real-time PCR (Applied Biosystems,
518 Foster City, CA, USA) using SYBR Premix Ex Taq (TaKaRa) and primers were listed
519 in Supplementary Table 9. The housekeeping *recA* gene of *H. alimentaria* EF61 was

used as a reference control for sample normalization.

Metagenomic and metatranscriptome analysis

Ratified protein sequences of MddH listed in Supplementary Table 10, as well as ratified protein sequences of MddA from *Mycobacterium tuberculosis* H37Rv (NP_217755.1), *B. diazoefficiens* USDA 110 Blr1218 (NP_767858.1) and Blr5741 (NP_772381.1), *Pseudomonas* sp. GM41 (WP_008148420.1), *P. deceptionensis* M1T (AJE75769) and *Sulfurovum* sp. NBC37-1 (YP_001358232.1)[8] were used as query sequences to perform hidden Markov Model (HMM)-based searches (HMMER 3.1b2) for homologs in seawater metagenome and metatranscriptome data using Ocean Gene Atlas[62], as well as in marine sediment metagenomic data from Bohai Sea and Yellow Sea[39] and soil metagenomes[41]. The cut-off E-value for HMM searches were set as <1e-80. The Tara Oceans Microbiome Reference Gene Catalog (OM-RGCv1) database containing data from 243 Tara Oceans samples was chosen to analyze the abundance of *mddH* and *mddA* in seawater metagenomes[36]. Cell numbers were estimated by the observed median abundance of ten prokaryotic single marker genes[36], and the abundance of *mddH* and *mddA* in metagenome data was normalized by cell number in each sample. The Tara Oceans Viromes data were obtained from iVirus (https://www.ivirus.us/data), and MddH homologs were identified by HMM searches with E-value <1e-80. The metagenomes from the Bohai and Yellow Sea sediment samples (top 5 cm surface sediment) were collected, sequenced and analyzed by Song et al.[39]. The metagenomes from rhizosphere soil samples of *Glycine soja*, *Sesbania cannabina* and *Sorghum bicolor* were collected, sequenced and analyzed by Zheng et

al.[41]. For the Bohai and the Yellow Sea sediment metagenome[47] and soil metagenome data[41], the relative abundances of *mddH* and *mddA* were calculated by normalizing to *recA* abundance, using a cut-off of E < 1e−50, as described by Song et al.[39]. *mddH* and *mddA* transcript abundance were analyzed against the Tara Oceans Microbiome Reference Gene Catalog with arctic data (OM-RGCv2)[38] and normalized by percent of mapped read. The abundance of *dddP* and *dmdA* in *Tara* Oceans metagenomes/metatranscriptomes and sediment metagenomes were also evaluated as above with specific cut-off E-value and corresponding ratified proteins described by Song et al.[39].

Statistics and Reproducibility

All measurements of MeSH and DMS levels (in bacterial strains or enzyme assays) and RT-qPCR were based on the mean of three biological replicates per strain/condition tested, and the error bars indicate standard deviations. To identify statistically significant differences between standard and experimental conditions in supplementary Figure 6e, a two-sided independent Student's *t*-test was applied to the data. To compare the gene abundance between different groups in supplementary Fig. 7, statistical analysis was carried out in Origin Pro 2021 and the normality of data in each group were tested. Non-normally distributed data was compared by Mann-Whitney test (between two groups) or Kruskal-Wallis test (between three groups). For Figure 3a and supplementary Figure 3a, at least three independent experiments have been performed and the results shown were from one representative experiment. No statistical method

was used to predetermine sample size, and no data were excluded from the analyses.

Data availability

The genomes of six *Halomonas* strains were deposited in WGS Batch at NCBI under accession number JAMSHM000000000, JAMSHN000000000, JAMSHO000000000, JAMSHP000000000, CP098827 and CP098828 (PRJNA844217). The *ubiE* gene from *Vibrio* sp. ZXX013 was deposited at NCBI with accession number ON685883. Verified functional MddH protein sequences were listed in Supplementary Table 10. The Tara Oceans Microbiome Reference Gene Catalog (OM-RGCv1) database was obtained from Ocean Gene Atlas (https://tara-oceans.mio.osupytheas.fr/). The Tara Oceans Viromes data were obtained from iVirus (https://www.ivirus.us/data). Source data are provided with this paper.

Acknowledgement

This work was supported by the National Natural Science Foundation of China (92251303 and 32370118, Principal Investigator (PI): X.-H.Z.; 42376101, PI: Y.Z.), the Fundamental Research Funds for the Central Universities (202172002, PI: X.-H.Z.), the Scientific and Technological Innovation Project of Qingdao Marine Science and Technology Center (2022QNLM030004-3, LSKJ202203201 and LSKJ202203206, PI: X.-H.Z.), Biotechnology and Biological Sciences Research Council, UK (BB/X005968, PI: J.D.T.), Natural Environmental Research Council, UK (NE/P012671, NE/S001352, NE/V000756/1, NE/X000990 and NE/X014428, PI: J.D.T.), Leverhulme trust (RPG-

2020-413, PI: J.D.T.), and the Biotechnology and Biological Sciences Research Council, UK (BB/M00256X/1 and BB/S008942/1, PI: A.J.G.).

Contributions

X.-H.Z. and Y.Z. conceived the work; X.-H.Z., Y.Z. and J.T. designed experiments; Y.Z. performed bioinformatic analysis and with J.T. and X.-H.Z. wrote the manuscript; Y.Z., C.S., and Z.G. carried out most of the experiments; L.L. helped in construction of in-frame deletion mutant; K.S. and X.Z. assisted with bioinformatic analysis; A.J.G. analyzed the enzyme kinetic and structural data. Y.Zheng analyzed soil metagenomes. All authors edited and approved the manuscript.

Ethics declarations

Competing interests

The authors declare no competing interests.

601 **Table 1. Activity of diverse MddH proteins expressed in *E. coli*.**

Source Organism	MeSH	H_2S	
	nmol DMS h^{-1} per mg total protein	nmol MeSH h^{-1} per mg total protein	nmol DMS h^{-1} per mg total protein
Algiphilus aromaticivorans DG1253	59.27±1.70	12.15±0.85	16.62±1.84
Marinobacter litoralis Sw-45	56.35±12.98	23.99±3.68	32.78±1.98
Pseudomonas pelagia CL-AP6	69.91±1.73	35.27±3.66	10.99±1.11
Hyphomonas adhaerens MHS-3	52.06±3.80	10.82±1.40	9.62±0.86
Pyruvatibacter mobilis CGMCC_1.15125	24.54±2.54	9.02±0.91	6.90±0.44
Novosphingobium colocasiae KCTC_32255	148.40±20.17	59.79±3.61	21.73±1.38
Erythrobacter ramosus DSM_8510	10.20±2.08	3.41±0.60	2.92±0.35
Ramlibacter aquaticus LMG_30558	45.54±5.30	18.16±2.17	8.80±0.64
Caulobacter henricii CB4	58.89±2.66	21.44±1.78	11.28±0.24
Halomonas alimentaria EF61	46.36±3.95	14.43±1.47	10.27±0.20
Vibrio alginolyticus ZXX013	ND	ND	ND

602 The values for DMS or MeSH production are shown as Mean±SD for three biological replicates. ND, not detectable.

603

Figure 1. **Pathways to MeSH/DMS production and their activity in *Halomonas* strains**. a, A simplified schematic representation of MeSH and DMS-related metabolic pathways and enzymes, only showing the molecules which contain the sulfur component that ends up in DMS. Green and grey arrows/fonts predict pathways and enzymes in *Halomonas* strains with Mdd activity and those not, respectively. The *Halomonas* strains were predicted to cleave DMSP via DMSP lyase enzymes (DddD) and oxidise DMS to DMSO (via DdhA and not Tmm). They were not predicted to reduce DMSO to DMS and lacked homologues to known DMSO reductase enzymes (Dms, Dor). The *Halomonas* strains lacked the potential to demethylate DMSP (via DmdA), but contained DmdBC and AcuH which convert 3-methylmercaptopropionate (MMPA) to MeSH. The MddA isoform enzyme was absent in *Halomonas* strains used in this study. *Halomonas* strains were grown in MBM and the following assays conducted; b, MeSH and DMS production with 0.5 mM L-Met added; c, DMS production with 0.5 mM MeSH added; d, DMS production with 0.5 mM DMSP added; e, MeSH and DMS production with 0.5 mM MMPA added; f, MeSH and DMS production with 0.5 mM H_2S added. The values for DMS and MeSH production are shown as the mean ±SD for three biological replicates. No MeSH or DMS was detected in the blank MBM media control.

Figure 2. **Maximum-likelihood phylogenetic tree of MddH proteins**. The tree is drawn to scale, with branch lengths measured in the number of substitutions per site. The scale bar indicates 0.5 amino acid substitutions per site. Different coloured circles at the end of each branch indicate bacterial taxonomy (see Taxonomy Key). Different label colors indicate the source of the bacterial strain (see Source Key). Proteins with experimentally ratified Mdd activity are marked with a yellow star near the labels. MddH from *Halomonas alimentaria* EF61 is highlighted by a red star. A putative UbiE protein from *Vibrio* sp. with no Mdd activity was used as an out-group (shown in a black box).

Figure 3. Characterization of the MddH enzyme. a, SDS-PAGE of purified MddH; b, In vitro DMS and/or MeSH production by purified MddH with MeSH or H_2S as substrates. The units ($nmol \cdot mg^{-1} \cdot h^{-1}$) represent the nanomolar amount of DMS or MeSH produced by MddH per milligram per hour; c, The ability of MddH to S-methylate a range of substrates (as detailed) monitored by the formation of *S*-adenosyl homocysteine (SAH) from *S*-adenosyl methionine (SAM); d, The effect of EDTA addition on MddH activity; e, Michaelis-Menten curves of purified MddH for H_2S *S*-methylation and SAM; f, Michaelis-Menten curves of purified MddH for MeSH *S*-methylation and SAM. Initial rates were determined with 0.27 µM MddH (molecular weight: 24.24 kDa) and 0-2 mM SAM (1 mM MeSH/H_2S), or 0-2 mM MeSH/H_2S (1 mM SAM) at 45°C, pH 9 in 30 mins. Kinetic parameters for MddH were determined by non-linear fitting using the Michaelis-Menten equation in the form $v/[E] = k_{cat} \cdot [S]/(K_m + [S])$ based on the initial rates of DMS production (or DMS and MeSH production) in triplicate experiments. The values are shown as the mean ±SD.

Figure 4. **The abundance of *mdd* genes and/or transcripts in global seawaters and coastal sediments**. a, The relative abundance of *mddH* and *mddA* in Tara Oceans metagenome samples from OM-RGCv1 database (normalized by cell numbers); b, Taxonomic assignment of MddH and MddA sequences in Tara Oceans metagenome samples from OM-RGCv1 database; c, The relative abundance of *mddH* and *mddA* transcripts in Tara Oceans metatranscriptome samples from OM-RGCv2 database (normalized by percent of mapped reads); d, The relative abundance of *mddH* and *mddA* in sediment metagenome samples from the Yellow Sea and the Bohai Sea (normalized by cell numbers); e, Taxonomy assignment of MddH and MddA sequences from sediment metagenome samples from the Yellow Sea and the Bohai Sea.

References

1. Ksionzek, K. B. *et al.* Dissolved organic sulfur in the ocean: Biogeochemistry of a petagram inventory. *Science.* **354**, 456–459 (2016).
2. Kiene, R. P. & Bates, T. S. Biological removal of dimethyl sulphide from sea water. *Nature* **345**, 702–705 (1990).
3. Vallina, S. M. & Simó, R. Strong relationship between DMS and the solar radiation dose over the global surface ocean. *Science.* **315**, 506–508 (2007).
4. Sievert, S., Kiene, R. & Schulz-Vogt, H. The sulfur cycle. *Oceanography* **20**, 117–123 (2007).
5. Li, C. Y. *et al.* Dimethylsulfoniopropionate and its catabolites are important chemical signals mediating marine microbial interactions. *Trends Microbiol.* **31**, 992–994 (2023).
6. Zhang, X.-H. *et al.* Biogenic production of DMSP and its degradation to DMS—their roles in the global sulfur cycle. *Sci. China Life Sci.* **62**, 1296–1319 (2019).
7. Stets, E. G., Hines, M. E. & Kiene, R. P. Thiol methylation potential in anoxic, low-pH wetland sediments and its relationship with dimethylsulfide production and organic carbon cycling. *FEMS Microbiol. Ecol.* **47**, 1–11 (2004).
8. Carrión, O. *et al.* A novel pathway producing dimethylsulphide in bacteria is widespread in soil environments. *Nat. Commun.* **6**, 6579 (2015).
9. Li, C. Y. *et al.* Aerobic methylation of hydrogen sulfide to dimethylsulfide in diverse microorganisms and environments. *ISME J. 2023 178* **17**, 1184–1193 (2023).
10. Tanaka, H., Esaki, N. & Soda, K. Properties of l-methionine γ-lyase from *Pseudomonas ovalis*. *Biochemistry* **16**, 100–106 (1977).
11. Lomans, B. P. *et al.* Obligate sulfide-dependent degradation of methoxylated aromatic compounds and formation of methanethiol and dimethyl sulfide by a freshwater sediment isolate, *Parasporobacterium paucivorans* gen. nov., sp. nov. *Appl. Environ. Microbiol.* **67**, 4017–4023 (2001).
12. Schäfer, H., Myronova, N. & Boden, R. Microbial degradation of

dimethylsulphide and related C1-sulphur compounds: Organisms and pathways controlling fluxes of sulphur in the biosphere. *J. Exp. Bot.* **61**, 315–334 (2010).

13. Howard, E. C. *et al.* Bacterial taxa that limit sulfur flux from the ocean. *Science.* **314**, 649–652 (2006).
14. Kiene, R. P., Linn, L. J. & Bruton, J. A. New and important roles for DMSP in marine microbial communities. *J. Sea Res.* **43**, 209–224 (2000).
15. Reisch, C. R. *et al.* Novel pathway for assimilation of dimethylsulphoniopropionate widespread in marine bacteria. *Nature* **473**, 208–211 (2011).
16. Miyazaki, J. *et al.* Deepest and hottest hydrothermal activity in the Okinawa trough: The Yokosuka site at Yaeyama Knoll. *R. Soc. Open Sci.* **4**, 171570 (2017).
17. Wang, F. & Chapman, P. M. Biological implications of sulfide in sediment - A review focusing on sediment toxicity. *Environ. Toxicol. Chem.* **18**, 2526–2532 (1999).
18. Carrión, O. *et al.* Methanethiol-dependent dimethylsulfide production in soil environments. *ISME J.* **11**, 2379–2390 (2017).
19. Carrión, O. *et al.* Methanethiol and dimethylsulfide cycling in Stiffkey saltmarsh. *Front. Microbiol.* **10**, 1–15 (2019).
20. Maldonato, B. J., Russell, D. A. & Totah, R. A. Human METTL7B is an alkyl thiol methyltransferase that metabolizes hydrogen sulfide and captopril. *Sci. Rep.* **11**, 1–13 (2021).
21. Dalmasy, J. M. G. *et al.* The thiol methyltransferase activity of TMT1A (METTL7A) is conserved across species. *bioRxiv* 11.17.567538 (2023).
22. Williams, B. T. *et al.* Bacteria are important dimethylsulfoniopropionate producers in coastal sediments. *Nat. Microbiol.* **4**, 1815–1825 (2019).
23. Todd, J. D. *et al.* Molecular dissection of bacterial acrylate catabolism - unexpected links with dimethylsulfoniopropionate catabolism and dimethyl sulfide production. *Environ. Microbiol.* **12**, 327–343 (2010).
24. Alcolombri, U., Laurino, P., Lara-Astiaso, P., Vardi, A. & Tawfik, D. S. DddD

is a CoA-transferase/lyase producing dimethyl sulfide in the marine environment. *Biochemistry* **53**, 5473–5475 (2014).

25. Lee, P. T., Hsu, A. Y., Ha, H. T. & Clarke, C. F. A C-methyltransferase involved in both ubiquinone and menaquinone biosynthesis: Isolation and identification of the Escherichia coli ubiE gene. *J. Bacteriol.* **179**, 1748–1754 (1997).

26. Jumper, J. *et al.* Highly accurate protein structure prediction with AlphaFold. *Nature* **596**, 583–589 (2021).

27. Maier, T. H. P. Semisynthetic production of unnatural L-α-amino acids by metabolic engineering of the cysteine- biosynthetic pathway. *Nat. Biotechnol.* **21**, 422–427 (2003).

28. Kessler, D. Enzymatic activation of sulfur for incorporation into biomolecules in prokaryotes. *FEMS Microbiol. Rev.* **30**, 825–840 (2006).

29. Midilli, A., Ay, M., Kale, A. & Veziroglu, T. N. A parametric investigation of hydrogen energy potential based on H_2S in Black Sea deep waters. *Int. J. Hydrogen Energy* **32**, 117–124 (2007).

30. Gros, V. *et al.* Concentrations of dissolved dimethyl sulfide (DMS), methanethiol and other trace gases in context of microbial communities from the temperate Atlantic to the Arctic Ocean. *Biogeosciences* **20**, 851–867 (2023).

31. Mironov, A. *et al.* CydDC functions as a cytoplasmic cystine reductase to sensitize Escherichia coli to oxidative stress and aminoglycosides. *Proc. Natl. Acad. Sci. U. S. A.* **117**, 23565–53570 (2020).

32. Mironov, A. *et al.* Mechanism of H_2S-mediated protection against oxidative stress in *Escherichia coli*. *Proc. Natl. Acad. Sci. U. S. A.* **114**, 6022–6027 (2017).

33. Bar-Even, A. *et al.* The moderately efficient enzyme: Evolutionary and physicochemical trends shaping enzyme parameters. *Biochemistry* **50**, 4402–4410 (2011).

34. Linder, D. P. & Rodgers, K. R. Methanethiol binding strengths and

750 deprotonation Energies in Zn(II)-imidazole complexes from M05-2X and MP2
751 theories: coordination number and geometry influences relevant to Zinc
752 enzymes. *J. Phys. Chem. B* **119**, 12182–12192 (2015).
753 35. Wilkening, J. V. *et al.* The production and fate of volatile organosulfur
754 compounds in sulfidic and ferruginous sediment. *J. Geophys. Res.*
755 *Biogeosciences* **124**, 3390–3402 (2019).
756 36. Sunagawa, S. *et al.* Structure and function of the global ocean microbiome.
757 *Science.* **348**, 1261359 (2015).
758 37. Brum, J. R. *et al.* Patterns and ecological drivers of ocean viral communities.
759 *Science.* **348**, 1261498 (2015).
760 38. Salazar, G. *et al.* Gene expression changes and community turnover
761 differentially shape the global ocean metatranscriptome. *Cell* **179**, 1068-
762 1083.e21 (2019).
763 39. Song, D. *et al.* Metagenomic insights into the cycling of
764 dimethylsulfoniopropionate and related molecules in the Eastern China
765 Marginal Seas. *Front. Microbiol.* **11**, 157 (2020).
766 40. Kallmeyer, J., Pockalny, R., Adhikari, R. R., Smith, D. C. & D'Hondt, S.
767 Global distribution of microbial abundance and biomass in subseafloor
768 sediment. *Proc. Natl. Acad. Sci. U. S. A.* **109**, 16213–16216 (2012).
769 41. Zheng, Y. *et al.* Patterns in the microbial community of salt-tolerant plants and
770 the functional genes associated with salt stress alleviation. *Microbiol. Spectr.* **9**,
771 1–15 (2021).
772 42. Whitman, W. B., Coleman, D. C. & Wiebe, W. J. Prokaryotes: The unseen
773 majority. *Proc. Natl. Acad. Sci. U. S. A.* **95**, 6578–6583 (1998).
774 43. Tuite, N. L., Fraser, K. R. & O'Byrne, C. P. Homocysteine toxicity in
775 *Escherichia coli* is caused by a perturbation of branched-chain amino acid
776 biosynthesis. *J. Bacteriol.* **187**, 4362–4371 (2005).
777 44. Curson, A. R. J. *et al.* Dimethylsulfoniopropionate biosynthesis in marine
778 bacteria and identification of the key gene in this process. *Nat. Microbiol.* **2**,
779 17009 (2017).

780 45. Sun, Y. *et al.* Adaption to hydrogen sulfide-rich environments: Strategies for
781 active detoxification in deep-sea symbiotic mussels, *Gigantidas platifrons*. *Sci.*
782 *Total Environ.* **804**, 150054 (2022).
783 46. Itoh, N. *et al.* Involvement of S-adenosylmethionine-dependent halide/thiol
784 methyltransferase (HTMT) in methyl halide emissions from agricultural plants:
785 Isolation and characterization of an HTMT-coding gene from *Raphanus sativus*
786 (daikon radish). *BMC Plant Biol.* **9**, 1–10 (2009).
787 47. Curson, A. R. J., Todd, J. D., Sullivan, M. J. & Johnston, A. W. B. Catabolism
788 of dimethylsulphoniopropionate: Microorganisms, enzymes and genes. *Nat.*
789 *Rev. Microbiol.* **9**, 849–859 (2011).
790 48. Kiene, R. P. & Linn, L. J. The fate of dissolved dimethylsulfoniopropionate
791 (DMSP) in seawater: Tracer studies using 35S-DMSP. *Geochim. Cosmochim.*
792 *Acta* **17**, 2797–2810 (2000).
793 49. Nightingale, P. D. & Liss, P. S. Gases in Seawater. *Treatise on Geochemistry*
794 **6–9**, 1–33 (2003).
795 50. Liu, J. *et al.* Bacterial dimethylsulfoniopropionate biosynthesis in the east china
796 sea. *Microorganisms* **9**, 1–22 (2021).
797 51. Seemann, T. Prokka: rapid prokaryotic genome annotation. *Bioinformatics* **30**,
798 2068–2069 (2014).
799 52. Brettin, T. *et al.* RASTtk: A modular and extensible implementation of the
800 RAST algorithm for building custom annotation pipelines and annotating
801 batches of genomes. *Sci. Rep.* **5**, 1–6 (2015).
802 53. Contreras-Moreira, B. & Vinuesa, P. GET_HOMOLOGUES, a Versatile
803 software package for scalable and robust microbial pangenome analysis. *Appl.*
804 *Environ. Microbiol.* **79**, 7696 (2013).
805 54. Zhang, S. H., Yang, G. P., Zhang, H. H. & Yang, J. Spatial variation of
806 biogenic sulfur in the south Yellow Sea and the East China Sea during summer
807 and its contribution to atmospheric sulfate aerosol. *Sci. Total Environ.* **488–**
808 **489**, 157–167 (2014).
809 55. Kumar, S., Stecher, G. & Tamura, K. MEGA7: Molecular evolutionary

genetics analysis version 7.0 for bigger datasets. *Mol. Biol. Evol.* **33**, 1870 (2016).

56. Nguyen, L. T., Schmidt, H. A., Von Haeseler, A. & Minh, B. Q. IQ-TREE: A fast and effective stochastic algorithm for estimating maximum-likelihood phylogenies. *Mol. Biol. Evol.* **32**, 268–274 (2015).

57. Letunic, I. & Bork, P. Interactive Tree Of Life (iTOL) v4: recent updates and new developments. *Nucleic Acids Res.* **47**, W256–W259 (2019).

58. Teufel, F. *et al.* SignalP 6.0 predicts all five types of signal peptides using protein language models. *Nat. Biotechnol.* **40**, 1023–1025 (2022).

59. Yu, C. S. *et al.* CELLO2GO: A web server for protein subcellular localization prediction with functional gene ontology annotation. *PLoS One* **9**, e99368 (2014).

60. Yu, N. Y. *et al.* PSORTb 3.0: Improved protein subcellular localization prediction with refined localization subcategories and predictive capabilities for all prokaryotes. *Bioinformatics* **26**, 1608–1615 (2010).

61. He, X. *et al.* Characterization of multiple alginate lyases in a highly efficient slginate-degrading *Vibrio* strain and its degradation strategy. *Appl. Environ. Microbiol.* **88**, e0138922 (2022).

62. Villar, E. *et al.* The Ocean Gene Atlas: exploring the biogeography of plankton genes online. *Nucleic Acids Res.* **46**, W289–W295 (2018).

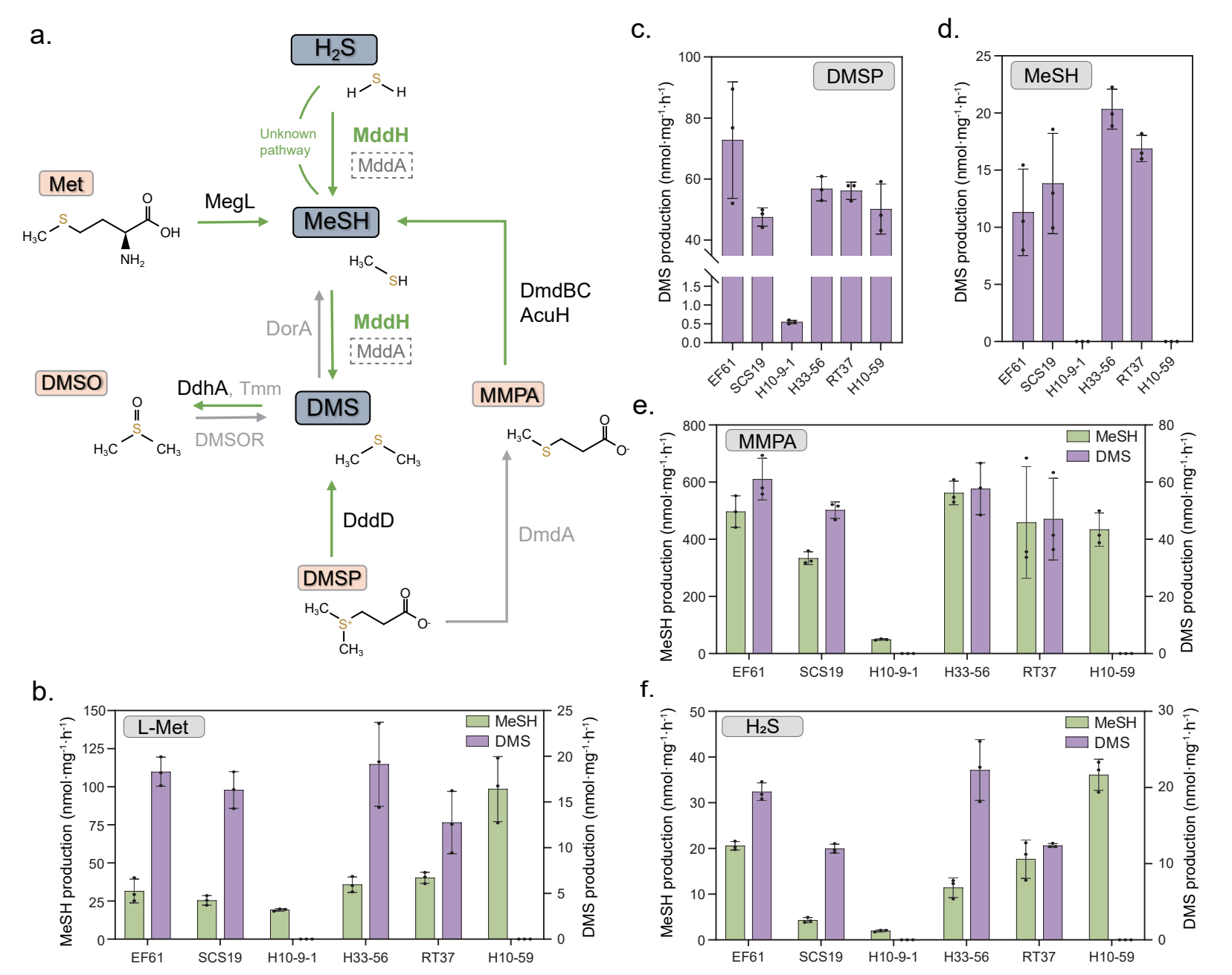
a.
H2S
Unknown pathway
MddH
MddA
Met
MegL
MeSH
DmdBC
AcuH
DorA
MddH
MddA
DMSO
DdhA, Tmm
DMSOR
DMS
MMPA
DddD
DmdA
DMSP
b.
L-Met
MeSH
DMS
MeSH production (nmol·mg⁻¹·h⁻¹)
DMS production (nmol·mg⁻¹·h⁻¹)
EF61
SCS19
H10-9-1
H33-56
RT37
H10-59
c.
DMSP
DMS production (nmol·mg⁻¹·h⁻¹)
d.
MeSH
e.
MMPA
f.
H2S

Tree scale: 0.5

Taxonomy Key

- *Alphaproteobacteria*
- *Betaproteobacteria*
- *Hydrogenophilalia*
- *Gammaproteobacteria*
- *Deltaproteobacteria*
- *Bacteroidetes*
- *Acidobacteria*

Sources

- Marine environment
- Soil environment
- Fresh water, lake, spring
- Other

WP 189621457.1 Novosphingobium colocasiae
WP 135245802.1 Polymorphobacterium henricii
WP 110450660.1 Phenylobacterium parvum
WP 062144739.1 Caulobacter fuscus
WP 006968164.1 Desulfotignum phosphitoxidans
WP 201588053.1 Psychrobacter jeotgali
WP 115384019.1 Jannaschia formosa
WP 109649093.1 Maribacter polysiphoniae
WP 099153359.1 Flaviliitoribacter nigricans
WP 009020202.1 Luminiphilus syltensis
WP 202060976.1 Microvirga aerilata
WP 188609420.1 Chelatococcus reniformis
WP 145770126.1 Denitratisoma oestradiolicum
WP 213163041.1 Kaustia mangrovi
WP 132706416.1 Rhodothalassium salexigens
WP 045218589.1 Desulfonatronum thioautotrophicum
Vibrio sp.
WP 119584011.1 Aurantiacibacter zhengii
WP 057883155.1 Tsuneonella troitsensis
WP 061924246.1 Altererythrobacter epoxidivorans
WP 160761066.1 Erythrobacter ramosus
WP 069959359.1 Magnetovibrio blakemorei
WP 132937505.1 Varunaivibrio sulfuroxidans
WP 002625346.1 Cystobacter fuscus
WP 035357756.1 Edaphobacter aggregans
WP 147799461.1 Pelomicrobium methylotrophicum
WP 083024695.1 Halomonas lionensis
WP 048442352.1 Methylobacterium variabile
WP 040484852.1 Lutibaculum baratangense
WP 184334353.1 Povalibacter uvarum
WP 165030742.1 Mesorhizobium camelthorni
WP 005004498.1 Nitrococcus mobilis
WP 037340972.1 Salinisphaera hydrothermalis
WP 065729703.1 Bradyrhizobium icense
WP 106714032.1 Phyllobacterium brassicacearum
WP 151613313.1 Ensifer alkalisoli
WP 028000384.1 Sinorhizobium arboris
WP 026942281.1 Hellea balneolensis
WP 189584807.1 Litorimonas cladophorae
WP 189496264.1 Algimonas arctica
WP 138519042.1 Limnobacter alexandrii
WP 066093655.1 Hydrogenophaga crassostreae
WP 193782355.1 Ramlibacter aquaticus
WP 029525378.1 Polaromonas glacialis
WP 119290301.1 Calidifontimicrobium sediminis
WP 108313018.1 Limnohabitans parvus
WP 188418859.1 Oxalicibacterium solurbis
WP 138855636.1 Inhella inkyongensis
WP 028997089.1 Azohydromonas australica
WP 109718595.1 Abyssibacter profundi
WP 083560959.1 Oceanococcus atlanticus
WP 029921409.1 Nevskia soli
WP 043766208.1 Algiphilus aromaticivorans
WP 133883595.1 Panacagrimonas perspica
WP 029889402.1 Polycyclovorans algicola
WP 093287594.1 Solimonas aquatica
WP 202635784.1 Rugosibacter aromaticivorans
WP 072899514.1 Hydrocarboniphaga daqingensis
WP 107940011.1 Stenotrophobium rhamnosiphilum
WP 123210354.1 Stagnimonas aquatica
WP 110263829.1 Sinimarinibacterium flocculans
WP 091532013.1 Fontimonas thermophila
WP 088273135.1 Pseudomonas aestusnigri
WP 074941468.1 Pseudomonas composti
WP 150547550.1 Pseudomonas marincola
WP 160195615.1 Aequoribacter fuscus
WP 109907004.1 Zavarzinia aquatilis
WP 152217008.1 Parvibaculum sedimenti
WP 045444609.1 Tepidicaulis marinus
WP 123034478.1 Haliea alexandrii
WP 117953165.1 Halioglobus sediminis
WP 101521179.1 Kineobactrum sediminis
WP 023659608.1 Congregibacter litoralis
WP 035515313.1 Pseudohaliea rubra
WP 117316660.1 Chromatocurvus halotolerans
WP 191250033.1 Kordiimonas sediminis
WP 160588566.1 Pyruvatibacter mobilis
WP 031551854.1 Parvularcula oceani
WP 104829662.1 Marinicaulis flavus
WP 089411452.1 Amphiplicatus metriothermophilus
WP 123235118.1 Marmoricola solisilvae
WP 167095931.1 Amycolatopsis granulosa
WP 064438519.1 Hoyosella altamirensis
WP 072700596.1 Rhodococcus coprophilus
WP 006865237.1 Gordonia namibiensis
WP 211829914.1 Kistimonas asteriae
WP 087462641.1 Oleiphilus messinensis
WP 113954515.1 Arenicella xantha
WP 193189154.1 Microbulbifer taiwanensis
WP 091642787.1 Aquisalimonas asiatica
WP 136254915.1 Halomonas alimentaria EF61
WP 183383648.1 Halomonas niordiana
WP 167111596.1 Halomonas stenophila
WP 183409920.1 Halomonas bachuensis
WP 109261258.1 Litorivivens lipolytica
WP 022698501.1 Hyphobacterium indicum
WP 150022673.1 Euryhalocaulis caribicus
WP 022700509.1 Oceanicaulis alexandrii
WP 135994866.1 Alkalicaulis satellites
WP 188760491.1 Edaphobacter acidisoli
WP 022696219.1 Ponticaulis koreensis
WP 035568920.1 Hyphomonas adhaerens
WP 119454893.1 Henriciella algicola
WP 087112664.1 Parendozoicomonas haliclonae
WP 121049683.1 Sphingosinicella microcystinivorans
WP 136523704.1 Geomonas ferrireducens
WP 111496183.1 Marinobacter bohaiensis
WP 109825320.1 Leucothrix arctica
WP 041766278.1 Psychromonas ingrahamii
WP 148862741.1 Marinobacter fonticola
WP 204995004.1 Spongiibacter marinus
WP 103682649.1 Marortus luteolus
WP 184461481.1 Zhongshania antarctica
WP 116918423.1 Tamilnaduibacter salinus
WP 114333749.1 Marinobacter litoralis
WP 022964284.1 Pseudomonas pelagia
WP 104322658.1 Marinobacter maroccanus
WP 104271271.1 Marinobacter flavimaris

a.

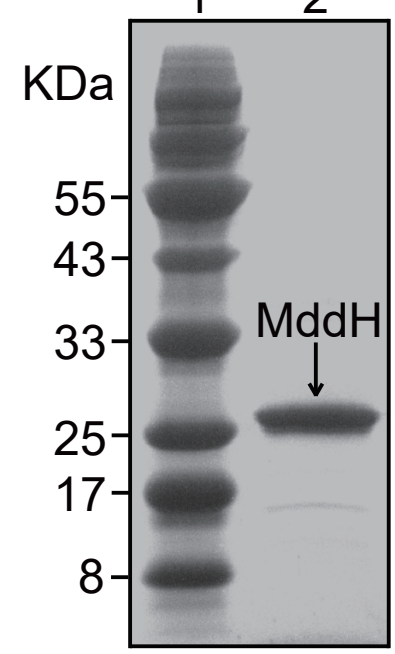
1
2
KDa
55
43
33
25
17
8
MddH

b.

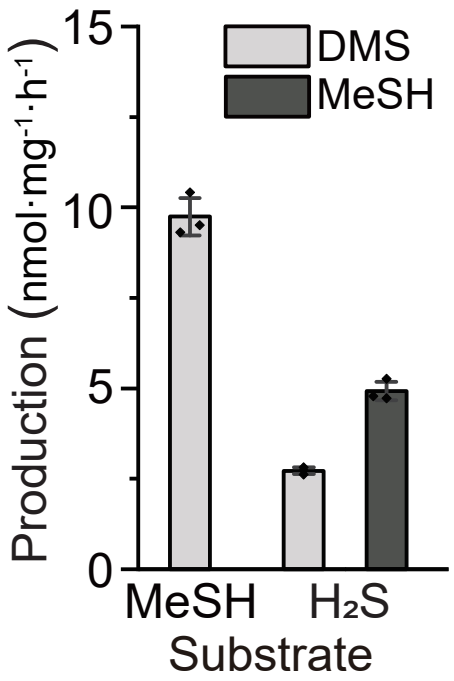
DMS
MeSH
Production (nmol·mg-1·h-1)
15
10
5
0
MeSH
H2S
Substrate

d.

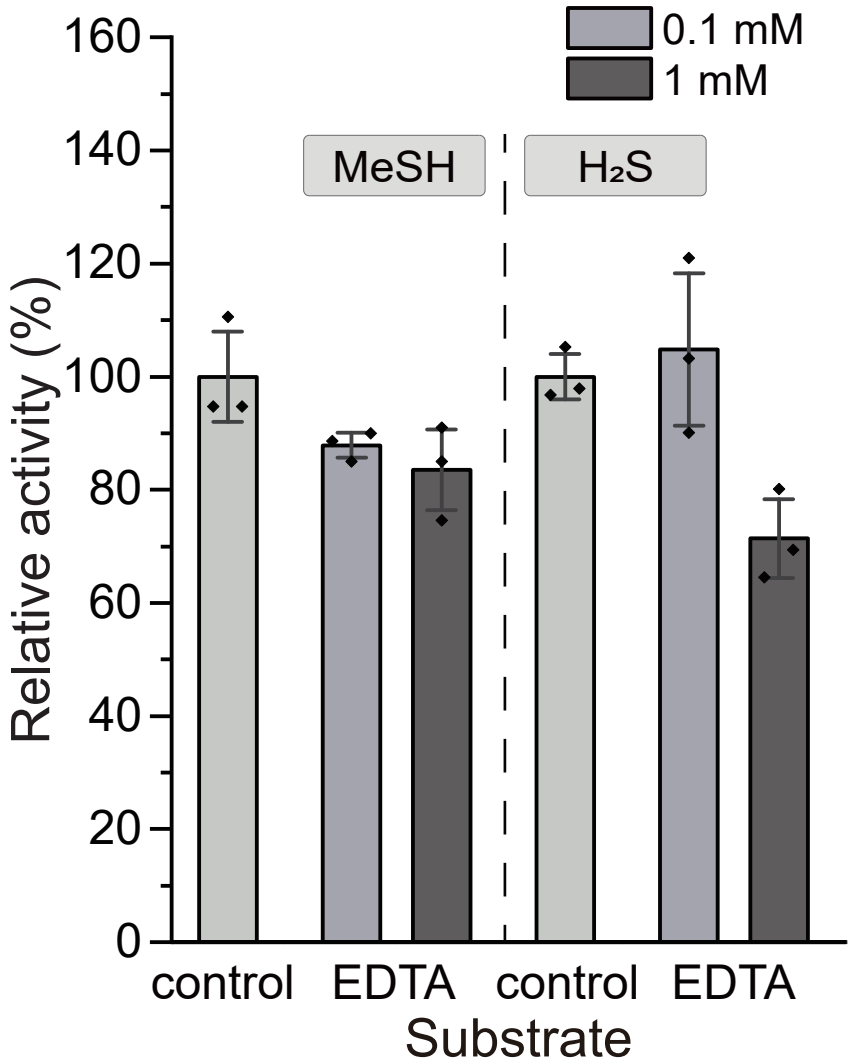
0.1 mM
1 mM
MeSH
H2S
Relative activity (%)
160
140
120
100
80
60
40
20
0
control
EDTA
control
EDTA
Substrate

c.

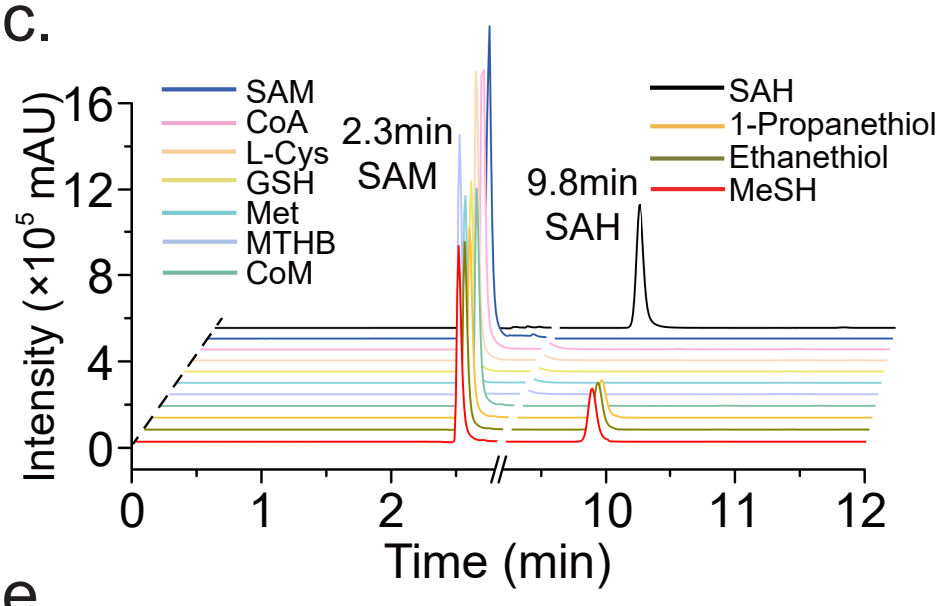
SAM
CoA
L-Cys
GSH
Met
MTHB
CoM
2.3min
SAM
9.8min
SAH
SAH
1-Propanethiol
Ethanethiol
MeSH
Intensity (×10^5 mAU)
16
12
8
4
0
0
1
2
10
11
12
Time (min)

e.

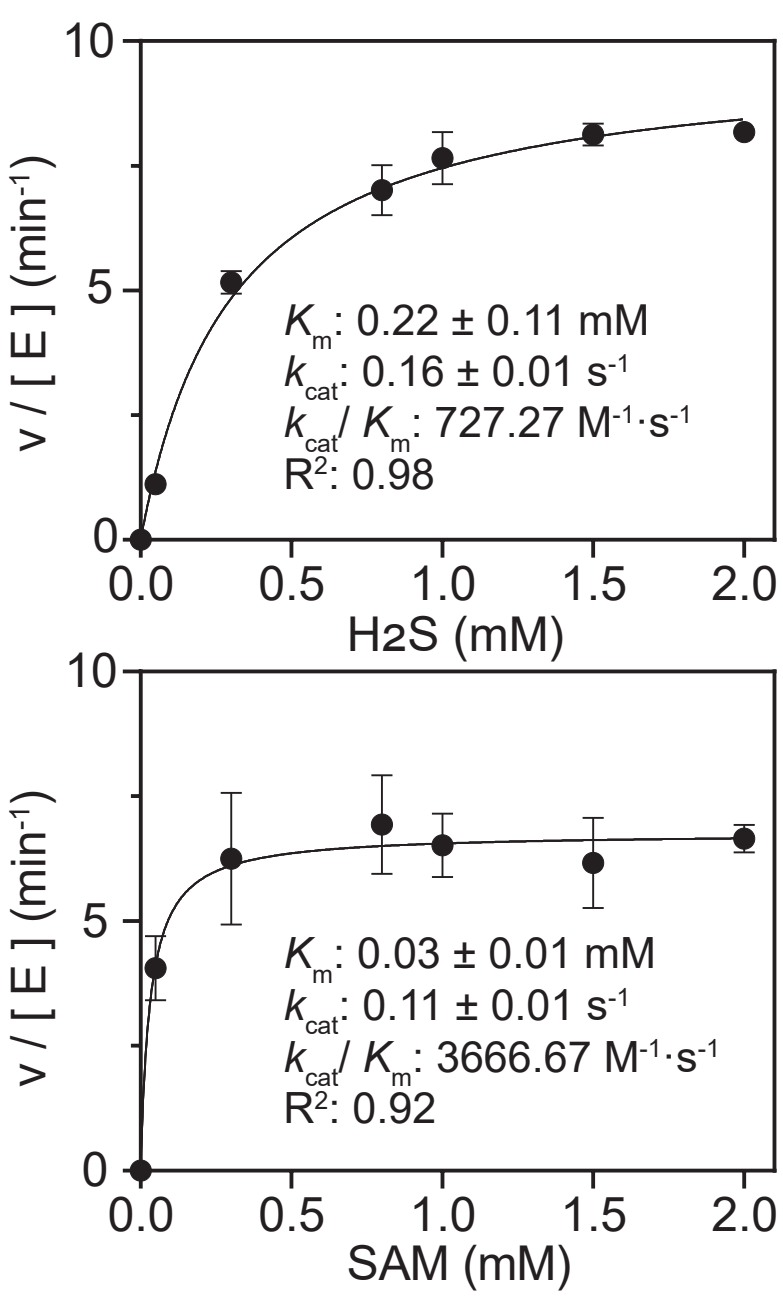
v / [E] (min-1)
10
5
0
Km: 0.22 ± 0.11 mM
kcat: 0.16 ± 0.01 s-1
kcat/ Km: 727.27 M-1·s-1
R2: 0.98
0.0
0.5
1.0
1.5
2.0
H2S (mM)
v / [E] (min-1)
10
5
0
Km: 0.03 ± 0.01 mM
kcat: 0.11 ± 0.01 s-1
kcat/ Km: 3666.67 M-1·s-1
R2: 0.92
0.0
0.5
1.0
1.5
2.0
SAM (mM)

f.

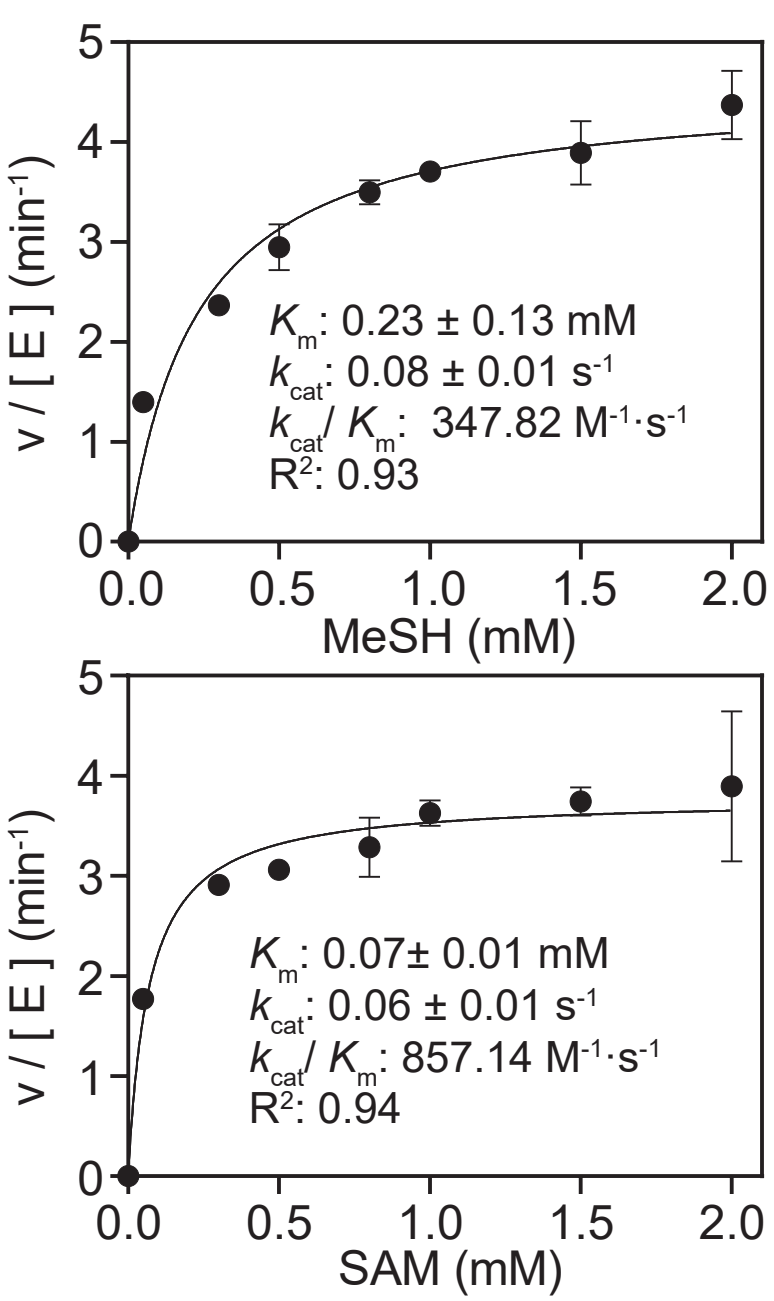
v / [E] (min-1)
5
4
3
2
1
0
Km: 0.23 ± 0.13 mM
kcat: 0.08 ± 0.01 s-1
kcat/ Km: 347.82 M-1·s-1
R2: 0.93
0.0
0.5
1.0
1.5
2.0
MeSH (mM)
v / [E] (min-1)
5
4
3
2
1
0
Km: 0.07± 0.01 mM
kcat: 0.06 ± 0.01 s-1
kcat/ Km: 857.14 M-1·s-1
R2: 0.94
0.0
0.5
1.0
1.5
2.0
SAM (mM)

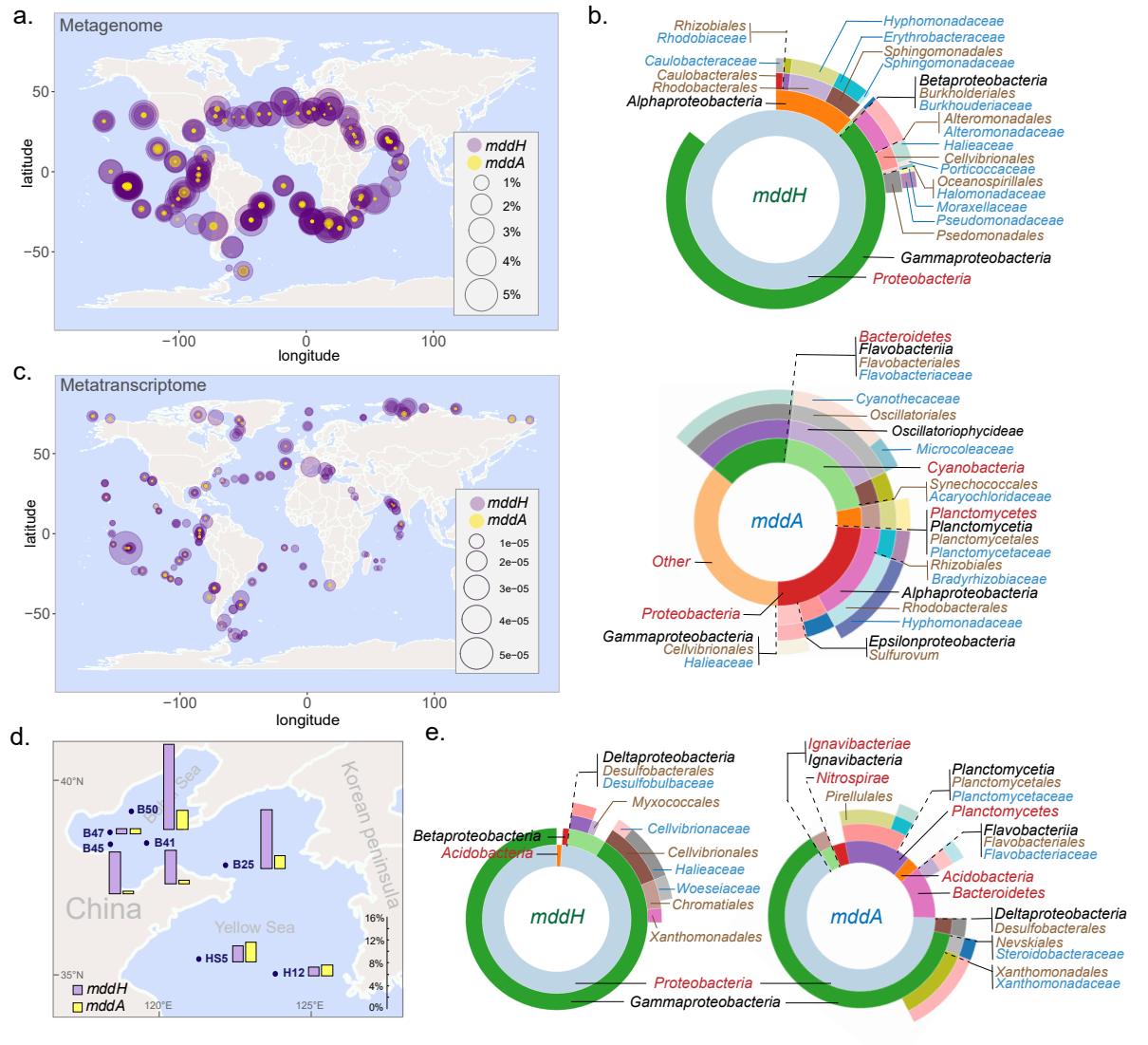
a.
Metagenome
latitude
longitude
mddH
mddA
1%
2%
3%
4%
5%
b.
Rhizobiales
Rhodobiaceae
Caulobacteraceae
Caulobacterales
Rhodobacterales
Alphaproteobacteria
Hyphomonadaceae
Erythrobacteraceae
Sphingomonadales
Sphingomonadaceae
Betaproteobacteria
Burkholderiales
Burkhouderiaceae
Alteromonadales
Alteromonadaceae
Halieaceae
Cellvibrionales
Porticoccaceae
Oceanospirillales
Halomonadaceae
Moraxellaceae
Pseudomonadaceae
Psedomonadales
Gammaproteobacteria
Proteobacteria
mddH
c.
Metatranscriptome
latitude
longitude
mddH
mddA
1e−05
2e−05
3e−05
4e−05
5e−05
Bacteroidetes
Flavobacteriia
Flavobacteriales
Flavobacteriaceae
Cyanothecaceae
Oscillatoriales
Oscillatoriophycideae
Microcoleaceae
Cyanobacteria
Synechococcales
Acaryochloridaceae
Planctomycetes
Planctomycetia
Planctomycetales
Planctomycetaceae
Rhizobiales
Bradyrhizobiaceae
Alphaproteobacteria
Rhodobacterales
Hyphomonadaceae
Epsilonproteobacteria
Sulfurovum
Other
Proteobacteria
Gammaproteobacteria
Cellvibrionales
Halieaceae
mddA
d.
40°N
35°N
120°E
125°E
China
Yellow Sea
Korean peninsula
B50
B47
B45
B41
B25
HS5
H12
mddH
mddA
16%
12%
8%
4%
0%
e.
Deltaproteobacteria
Desulfobacterales
Desulfobulbaceae
Myxococcales
Cellvibrionaceae
Betaproteobacteria
Acidobacteria
Cellvibrionales
Halieaceae
Woeseiaceae
Chromatiales
Xanthomonadales
Proteobacteria
Gammaproteobacteria
mddH
Ignavibacteriae
Ignavibacteria
Nitrospirae
Pirellulales
Planctomycetia
Planctomycetales
Planctomycetaceae
Planctomycetes
Flavobacteriia
Flavobacteriales
Flavobacteriaceae
Acidobacteria
Bacteroidetes
Deltaproteobacteria
Desulfobacterales
Nevskiales
Steroidobacteraceae
Xanthomonadales
Xanthomonadaceae
mddA

Supplementary information

An *S*-methyltransferase that produces the climate-active gas dimethylsulfide is widespread across diverse marine bacteria

Yunhui Zhang[1,2,3†], Chuang Sun[1†], Zihua Guo[1†], Liyan Liu[1], Xiaotong Zhang[1], Kai Sun[1], Yanfen Zheng[4], Andrew J. Gates[4], Jonathan D Todd[1,5*] and Xiao-Hua Zhang[1,2,3*]

*****Corresponding Author: Xiao-Hua Zhang, xhzhang@ouc.edu.cn; Jonathan D Todd, Jonathan.Todd@uea.ac.uk

This file includes:

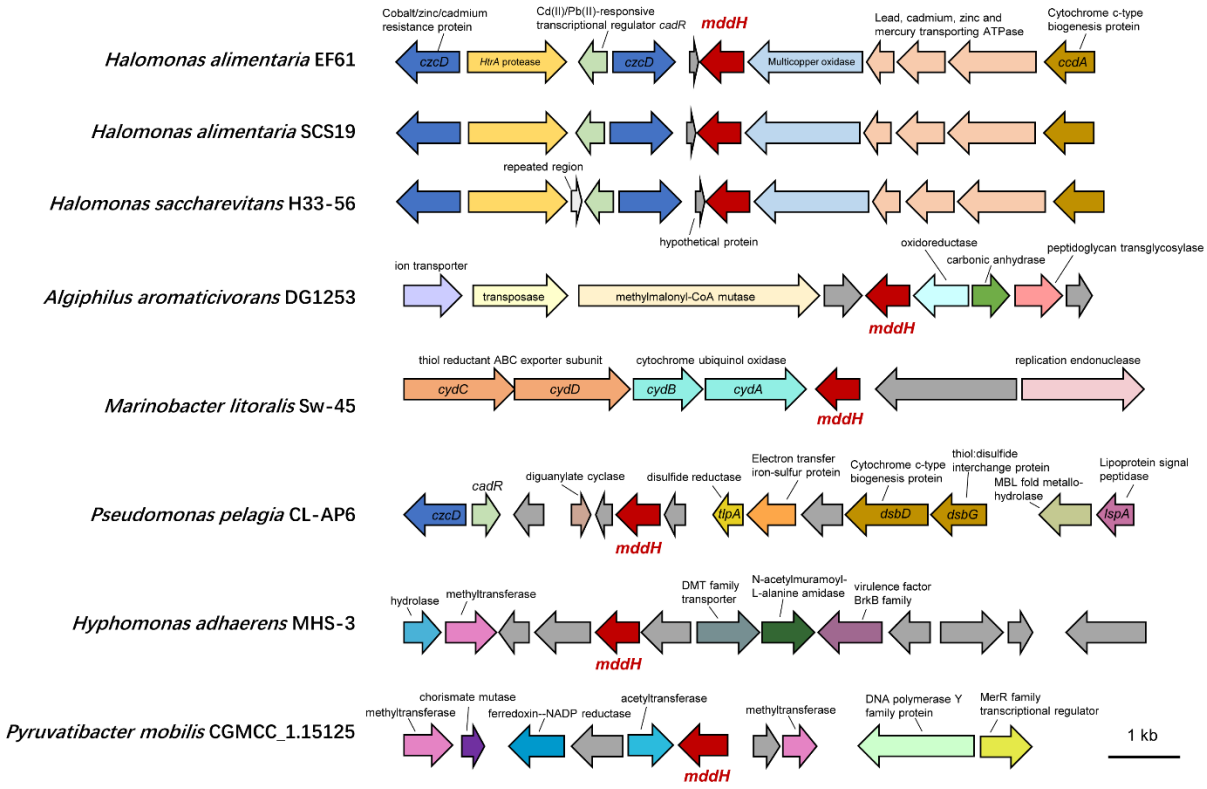

Supplementary Figure 1. The gene neighborhood of *mddH* in different bacteria. Genes are colour-coded and their predicted protein products are detailed near the arrows. Genes that encode hypothetical proteins are shown in grey. Scale bar indicates 1 kb of genomic DNA.

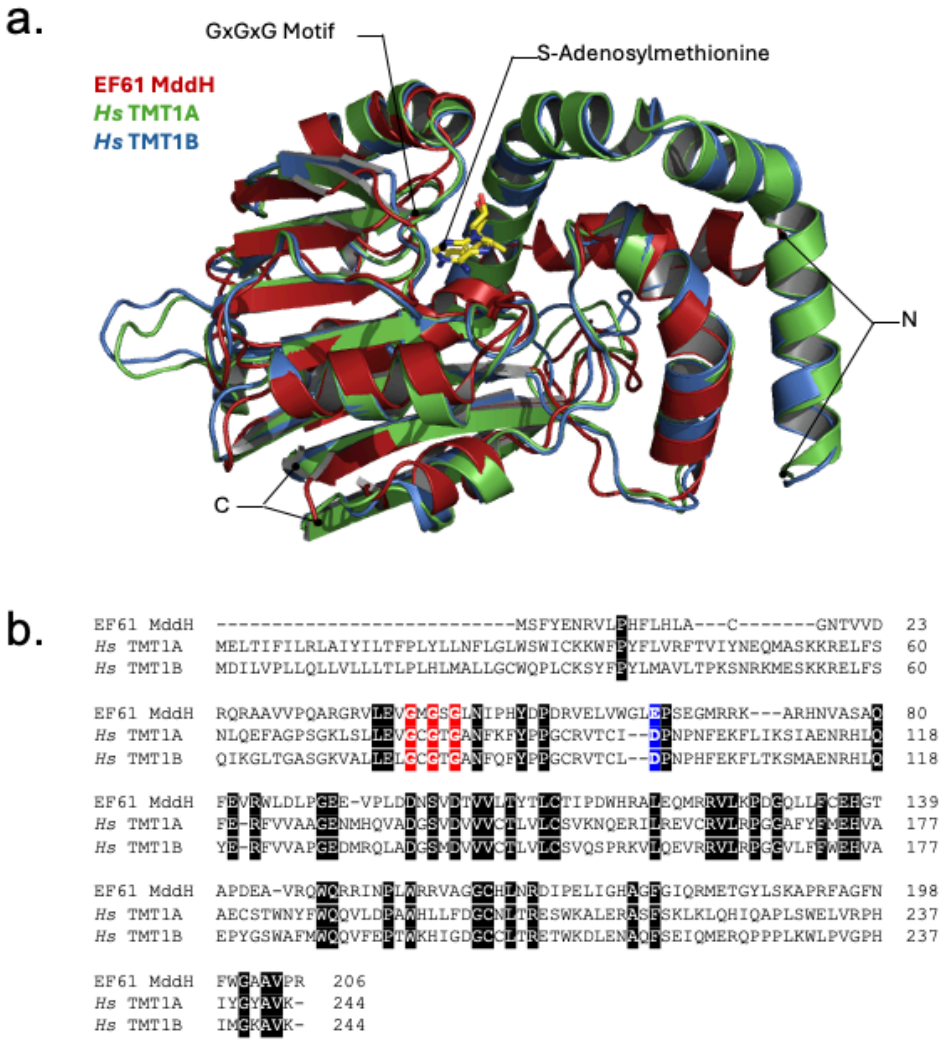

Supplementary Figure 2. Structural prediction of MddH using AlphaFold and comparison with other putative and known SAM-dependent methyltransferases. a) AlphaFold models for EF61 MddH (red) superpose with *Hs* TMT1A (green) and *Hs* TMT1B (blue) with RMSD values of 1.183 Å (125 Cα atoms) and 1.317 Å (131 Cα atoms), respectively. *S*-adenosylmethionine is modelled into EF61 MddH adjacent to the conserved GxGxG motif (https://www.biorxiv.org/content/10.1101/2023.11.17.567538v1) using the positional coordinates from the crystal structure of the related YcgJ protein from *Bacillus subitilis* (2GLU.pdb). The image was generated using Pymol ver 3.0.0. b) Multiple sequence alignment for MddH, TMT1A and TMT1B showing the conserved GxGxG motif (glycine residues highlighted in red) and a conserved acidic residue present in the SAM binding domain (Asp-93 for TMT1A/B and Glu-63 in MddH, highlighted in blue). Alignment was generated using Clustal Omega.

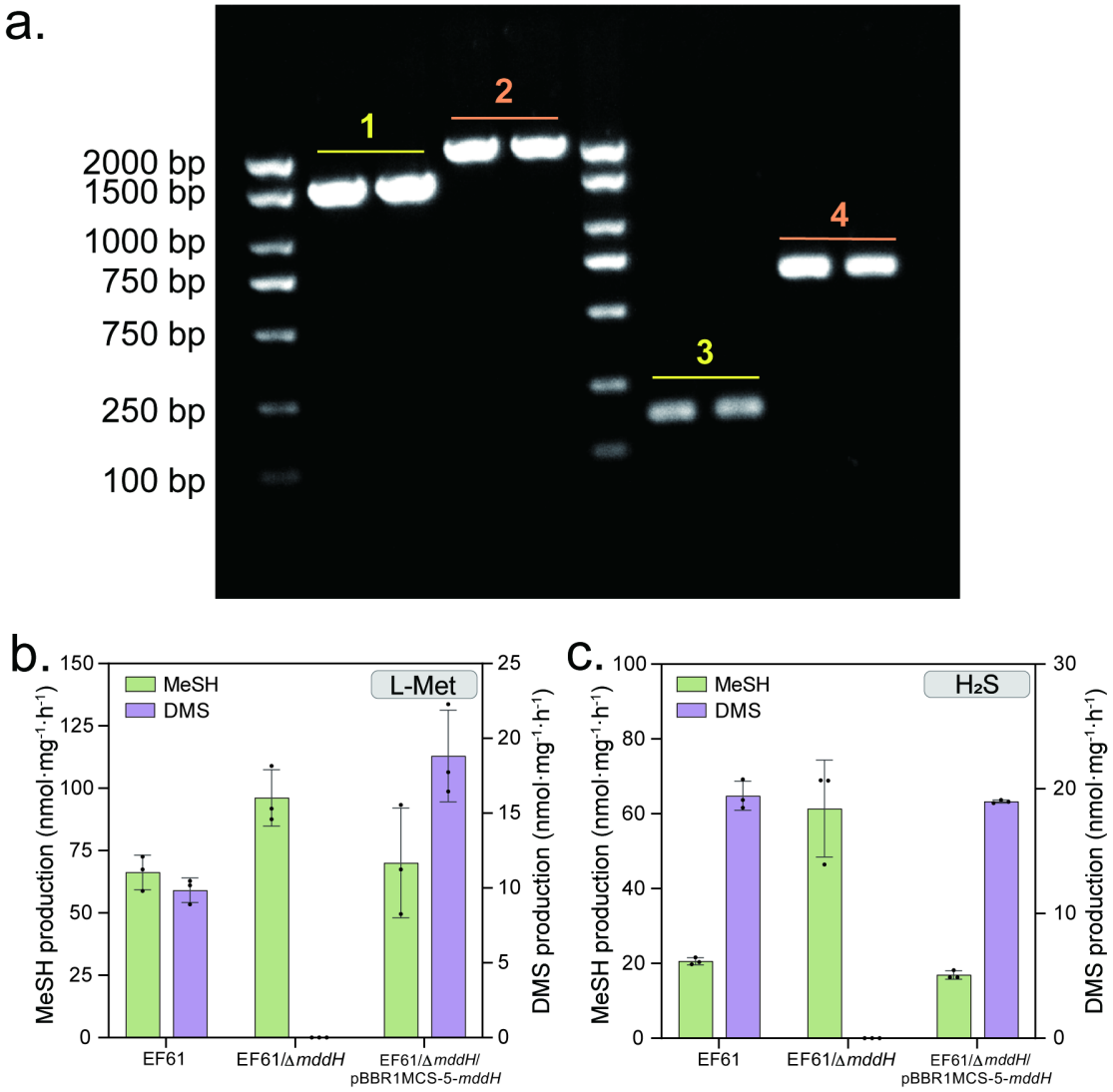

Supplementary Figure 3. PCR confirmation of the in-frame deletion within *H. alimentaria* EF61 *mddH* and MeSH and DMS production phenotypes of *H. alimentaria* EF61, Δ*mddH* mutant and the complemented strain. a, Amplification of DNA spanning the *mddH* region from the EF61/Δ*mddH* (fragment 1, predicted to be 1426 bp) and the wild type EF61 strains (fragment 2, predicted to be 1909 bp) using primers upstream (*mddH*-UO) and downstream (*mddH*-DO) of *mddH*. Amplification of the truncated and wild type *mddH* gene from the EF61/Δ*mddH* (fragment 3, predicted to be 137 bp) and the wild type EF61 strains (4, predicted to be 621 bp) using the MddHPE-F (N-terminal) and MddHPE-R (C-terminal) primers; b, MeSH and DMS production with 0.5 mM L-Met added; c, MeSH and DMS production with 0.5 mM H_2S added. The values for MeSH and DMS production are shown as the mean±SD of three biological replicates.

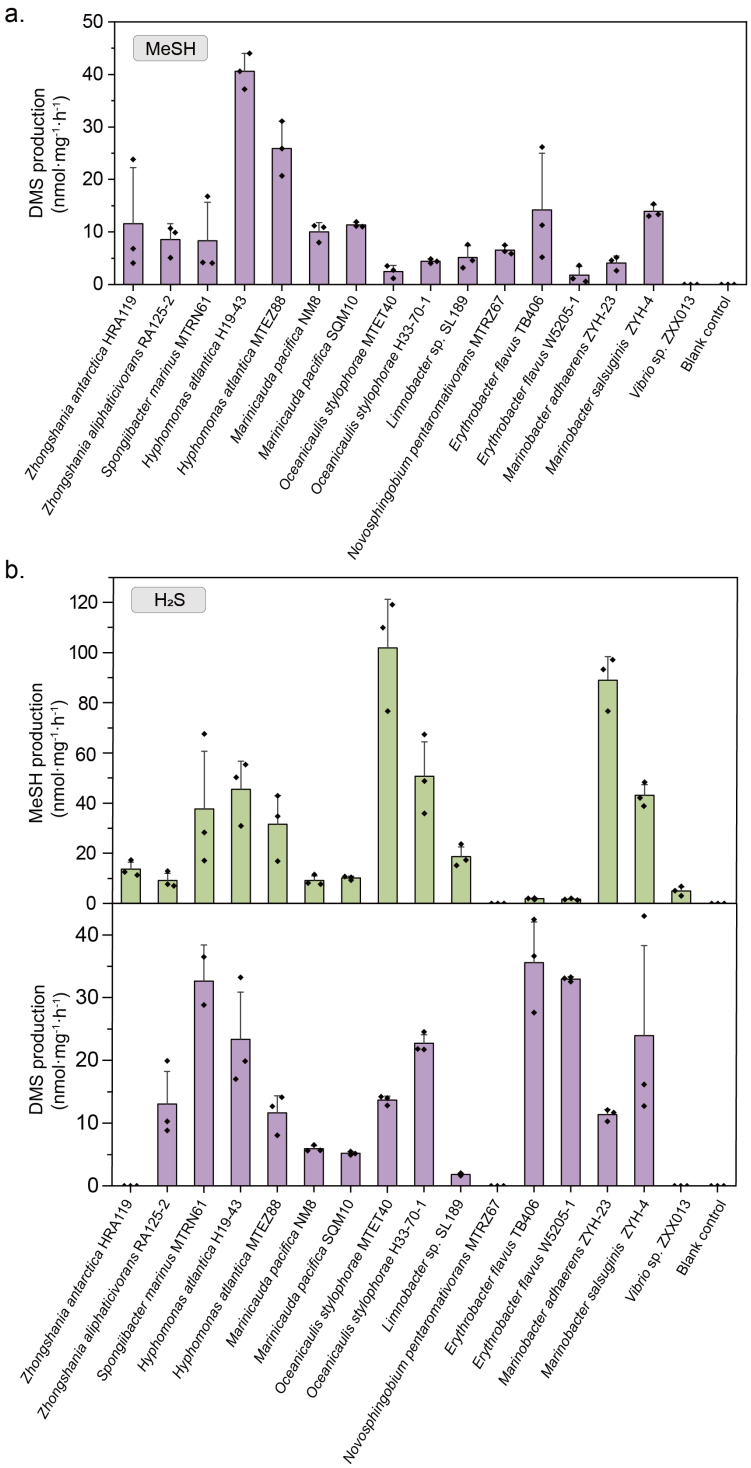

Supplementary Figure 4. The MeSH and H_2S *S*-methylation activities of representative marine bacterial isolates that possess MddH. a, DMS production from MeSH (0.5 mM); b, MeSH and DMS production from H_2S (0.5 mM). *Vibrio* sp. ZXX013 that lacks MddH and has no Mdd activity and media only controls were also included. The values for DMS production are shown as the mean ±SD of three biological replicates.

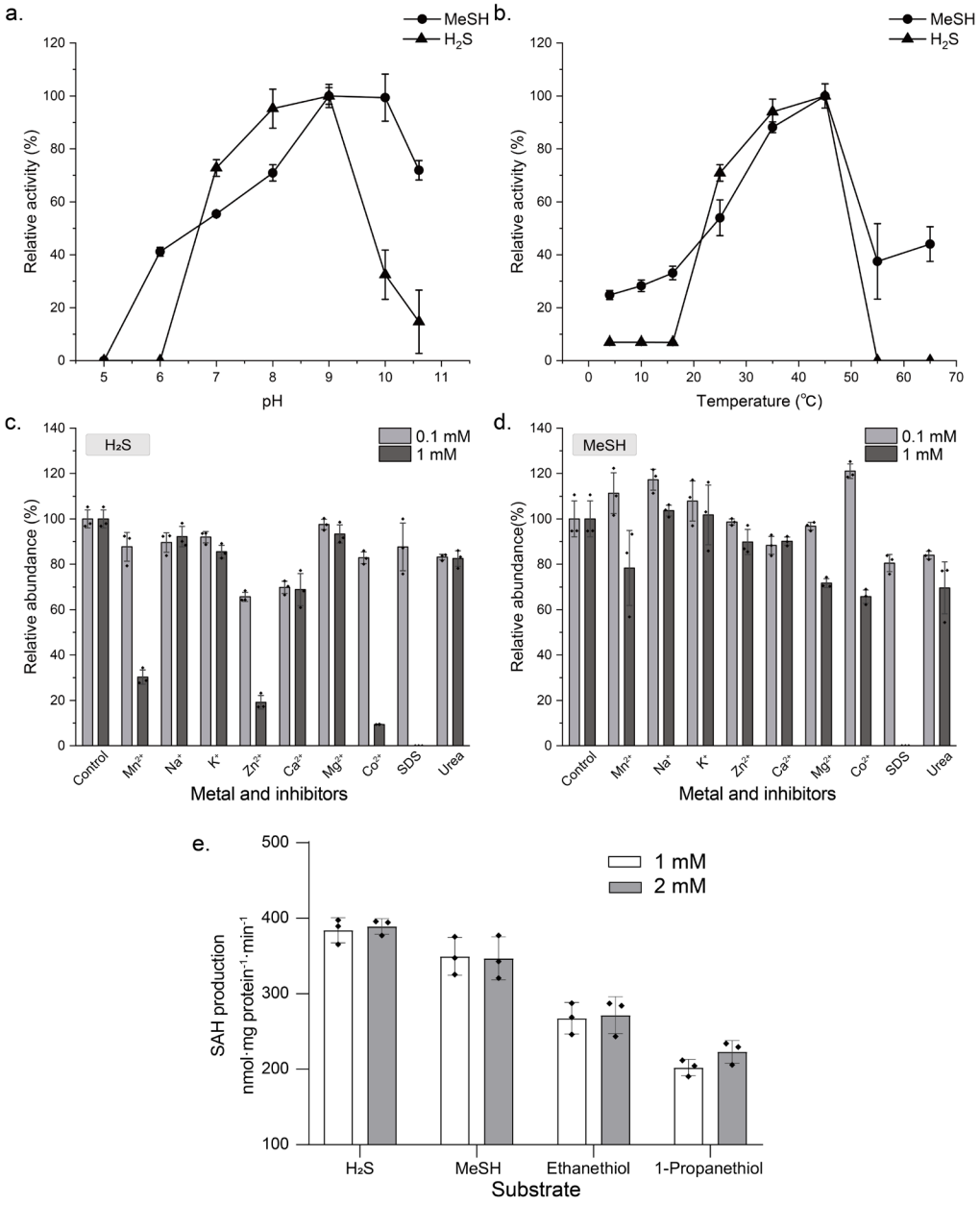

Supplementary Figure 5. Characterization of the MddH enzyme. a, MddH enzyme activity with MeSH and H_2S as substrates under different pH values; b, MddH enzyme activity using MeSH and H_2S as substrates under different temperatures; c-d, the effects of added metal ions on MddH activity when using MeSH (c) and H_2S (d) as substrates; e, in vitro SAH production by purified MddH with MeSH, H_2S, ethanethiol and 1-propanethiol as substrates. The values are shown as the mean ±SD of three biological replicates.

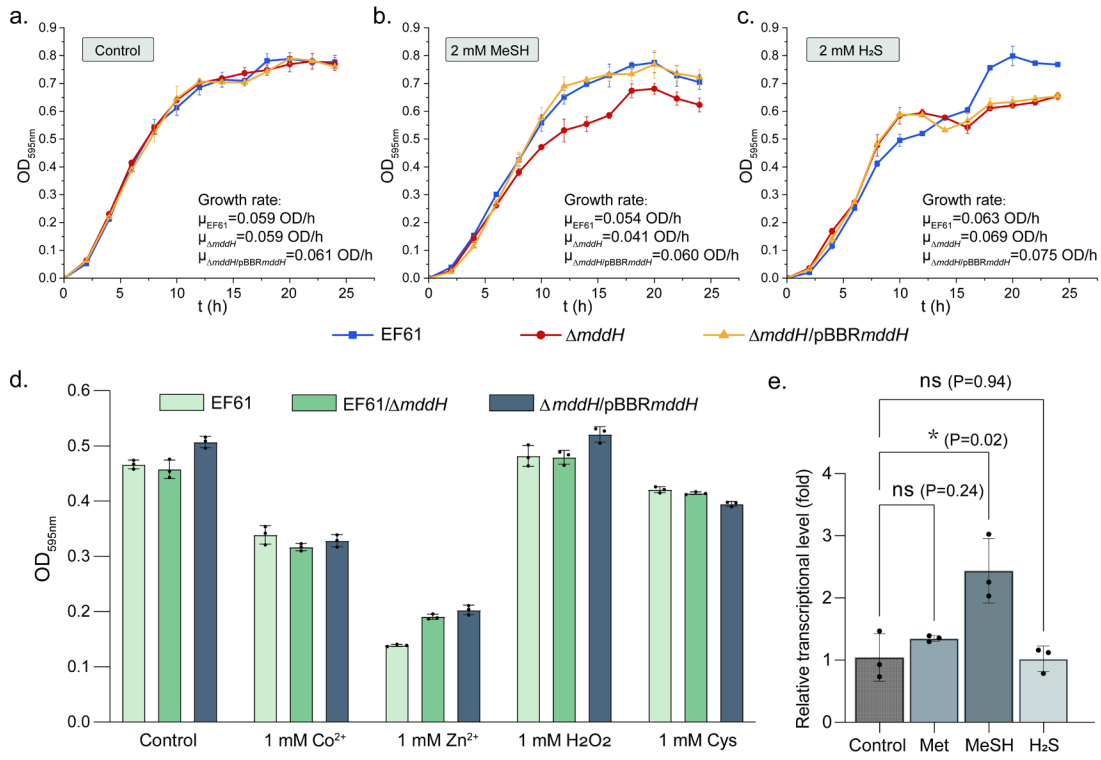

Supplementary Figure 6. Phenotypic experiments of *H. alimentaria* EF61, Δ*mddH* mutant and the complemented strain. a-c, Growth curve analysis of the *H. alimentaria* EF61, △*mddH* mutant and△*mddH* complemented strains in MBM medium without MeSH or H_2S as a control (a); or with 2 mM MeSH (b) 2 mM H_2S (c). The values for OD_{595nm} are shown as the mean±SD for three biological replicates. The initial growth rates during the exponential phase are indicated on each graph as μ (OD/h); d, end point growth analysis of the *H. alimentaria* EF61, EF61/△*mddH* mutant and *mddH* complemented strains with 1 mM Co^{2+}, Zn^{2+}, H_2O_2 and cysteine (indicated by end point OD_{595nm} levels). The values for OD_{595nm} are shown as the mean±SD for three biological replicates; e, RT-qPCR analysis of *mddH* transcript levels in *H. alimentaria* EF61 incubated with Met, MeSH or H_2S added at 1 mM levels. The Transcript levels are shown as the mean±SD for three biological replicates. *, $p<0.05$ in two-sided independent Student *t*-test; ns, not significant.

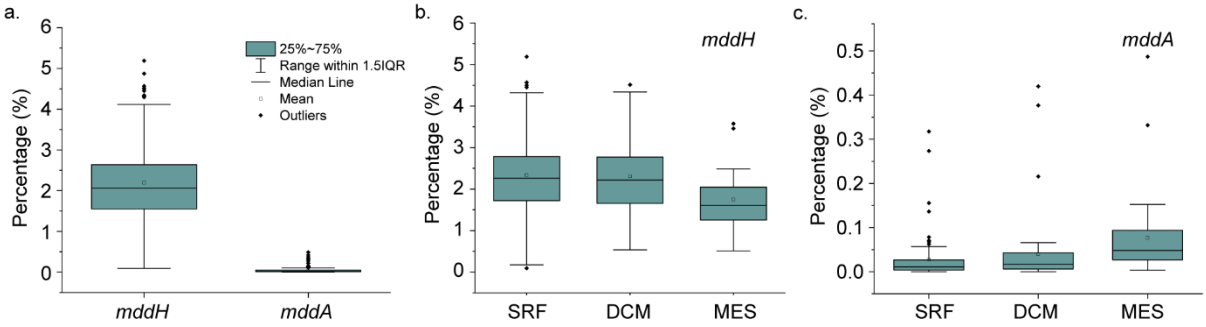

Supplementary Figure 7. The relative abundance of *mddH* and *mddA* in Tara Oceans metagenomes. a, The relative abundance of *mddH* and *mddA* in 178 samples of >0.22 μm fractions; b, The relative abundance of *mddH* in different water layers (SRF: 81 samples, DCM: 51 samples, MES: 36 samples); c, The relative abundance of *mddA* in different water layers (SRF: 81 samples, DCM: 51 samples, MES: 36 samples). Boxes span the 25%-75% range; the line within each box denotes the median, and whiskers indicate the extreme edges of the distribution as defined by values that are 1.5 times the interquartile range. SRF: surface water, DCM: deep chlorophyll maximum layers, MES: mesopelagic zone.

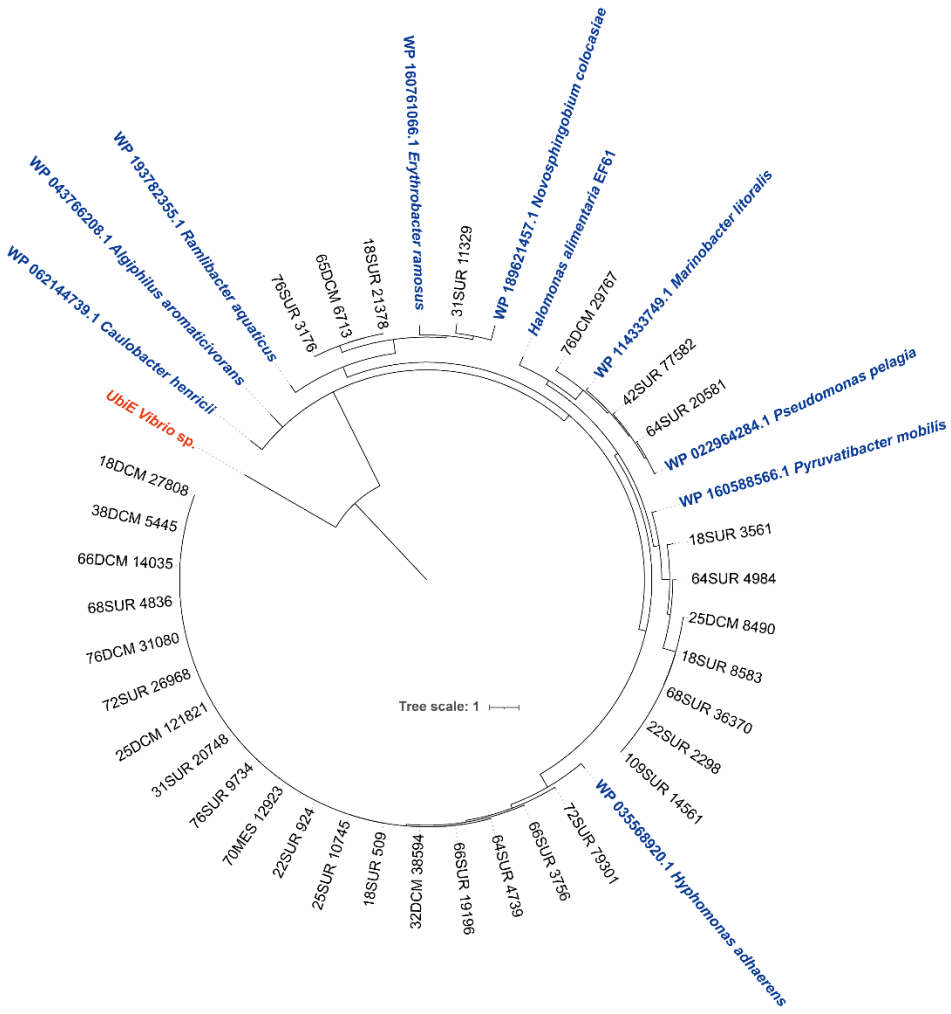

Supplementary Figure 8. Maximum-likelihood phylogenetic tree of functionally ratified bacterial MddH proteins and potential MddH homologs from Tara Oceans Viromes. The tree is built with LG+G4 model and is drawn to scale, with branch lengths measured in the number of substitutions per site. The scale bar indicates 1 amino acid substitutions per site. Blue label color indicates the functionally ratified bacterial MddH, and black ones indicate the MddH from Tara Oceans Virome. A putative UbiE protein from *Vibrio* sp. with no Mdd activity was used as an out-group.

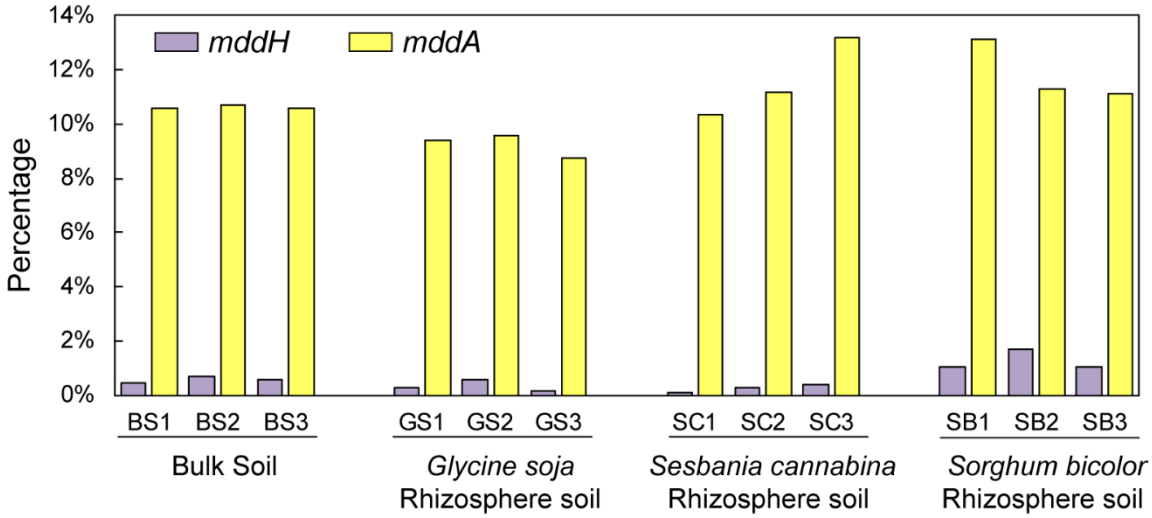

Supplementary Figure 9. The relative abundance of *mddA* and *mddH* in triplicate soil metagenomes from four different sources.

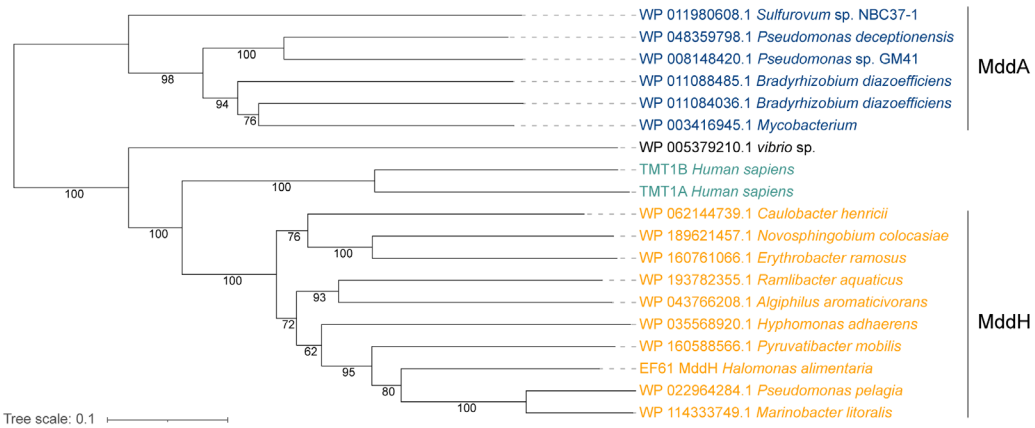

Supplementary Figure 10. Maximum-likelihood phylogenetic tree of functionally ratified MddA, MddH, TMT1A and TMT1B proteins. Functional MddA sequences (blue) were used as reference sequences. Yellow label color indicates the functionally ratified bacterial MddH proteins. The human TMT1A and TMT1B proteins are indicated in turquoise. A putative UbiE protein from *Vibrio* sp. with no Mdd activity was used as an out-group. The scale bar indicates 0.1 amino acid substitutions per site.

Supplementary Table 1. Strains used in this study.

Strain	Description
Halomonas alimentaria EF61	Isolated from seawater in the Mariana Trench
Halomonas alimentaria SCS19	Isolated from shrimp in the Okinawa Trough
Halomonas alimentaria H10-9-1	Isolated from seawater in the Yellow Sea
Halomonas saccharevitans H33-56	Isolated from seawater in the Yellow Sea
Halomonas saccharevitans RT37	Isolated from seawater of the Mariana Trench
Halomonas saccharevitans H10-59	Isolated from seawater in the Yellow Sea
E. coli JM101	Used to amplify pBluescript SKII(-) with flanking region of *mddH*
E. coli 803	Used to host pK18mocsacB and pRK2013
H. alimentaria EF61/Δ*mddH*	In-frame deletion mutant of *mddH*
E. coli BL21	Strain with T7 polymerase used to express cloned *mddH* genes
E. coli JM109	Clone strain used to host pUCm-T
Zhongshania aliphaticivorans RA125-2	Isolated from sediment in Okinawa Trough
Spongiibacter marinus MTRN61	Isolated from seawater of Mariana Trench
Hyphomonas atlantica H19-43	Isolated from seawater in the Yellow Sea
Hyphomonas atlantica MTEZ88	Isolated from seawater of the Mariana Trench
Marinicauda pacifica NM8	Isolated from seawater in the Okinawa Trough
Marinicauda pacifica SQM10	Isolated from seawater in the Okinawa Trough
Oceanicaulis stylophorae MTET40	Isolated from seawater of the Mariana Trench
Oceanicaulis stylophorae H33-70-1	Isolated from seawater in the Yellow Sea
Limnobacter sp. SL189	Isolated from seawater in the Nordic Sea
Erythrobacter flavus TB406	Isolated from seawater of the polumetallic nodule region
Erythrobacter flavus W5205-1	Isolated from seawater in the Okinawa Trough
Marinobacter adhaerens ZYH-23	Isolated from the sediment of the South China Sea
Marinobacter salsuginis ZYH-4	Isolated from the sediment of the South China Sea
Vibrio sp. ZXX103	Isolated from seawater of the Mariana Trench. Non-DMS producing strain.

Supplementary Table 2. DMS production by *Halomonas alimentaria* EF61 when incubated in sterilized coastal seawater.

Conditions	DMS concentration (nM)	DMS (pmol·mg protein^{-1}·h^{-1})
4 nM MeSH+Seawater Control	0.392±0.109	-
4 nM H_2S + Seawater Control	0.237±0.061	-
4 nM MeSH + EF61	3.250±0.147	3.758±0.721
4 nM MeSH + EF61 Δ*mddH*	0.360±0.064	0.380±0.072
4 nM H_2S + EF61	2.057±0.249	2.645±0.489
4 nM H_2S + EF61 Δ*mddH*	0.373±0.134	0.516±0.198

Supplementary Table 3. Predicted homologues of MddH using the structural comparison server DALI (). The top 10 matches against the PDB25 database are shown using the Alphafold MddH model (Supplementary Figure 2a, red). Matches are ranked by Z-score and those with sequence identity of 20% or above are highlighted in grey.

PDB (Chain)	Z-Score	RMSD (Å)	% Seq. Identity	Organism	Description	Ref.
2GLU(A)	17.8	2.4	20	*Bacillus subitilis*	YcgJ, unknown function	-
7V6H(A)	17.6	2.5	15	*Saccharopolyspora spinosa*	SpnL, Cyclopropane fatty-acyl-phospholipid synthase-like methyltransferase	[1]
6F5Z(B)	17.4	2.9	19	*Haloferax volcanii* DS2	Hvo_0019, 24-Sterol C-methyltransferase	[2]
3OFK(A)	17.0	2.5	11	*Bradyrhizobium* sp. WM9	NodS, N-methyltransferase	[3]
3MGG(B)	16.9	3.1	21	*Methanosarcina mazei*	Putative methyltransferase	-
2O57(A)	16.8	2.9	14	*Galdieria sulphuraria*	Putative sarcosine dimethylglycine methyltransferase	-
3SM3(A)	16.8	2.9	20	*Methanosarcina mazei* Go1	MaR262, Putative SAM-dependent methyltransferase	-
4OBW(C)	16.6	3.3	16	*Saccharomyces cerevisiae* S288C	Coq5, C- methyltransferase	[4]
5GM2(B)	16.5	2.8	20	*Streptomyces blastmyceticus*	TleD, SAM-dependent methyltransferase	[5]
5UFM(A)	16.3	3.0	15	*Burkholderia thailandensis* E264	*Bth*II1283, 1,6-Didesmethyltoxoflavin N-Methyltransferase	[6]

Supplementary Table 4. The abundance of Mdd genes and major DMSP catabolic genes in Tara Ocean samples.

	mddH	*mddA*	*dddP*	*dmdA*
Metagenome (per cell)	0.09%-5.2% (average: 2.19 ± 0.93%)	0.0007%-0.4% (average: 0.04±0.07%)	0.4%-29.3% (average: 12.4% ± 6.7%)	1.7%-40.3% (average: 19.5% ± 11.5%)
Transcriptome (per mapped read)	2.80×10^{-7}-5.33×10^{-5}	4.84×10^{-9}-8.03×10^{-7}	2.78×10^{-7}-9.98×10^{-5}	6.44×10^{-7}-1.54×10^{-4}

Supplementary Table 5. MddH homologous sequences identified in Tara Oceans Virome and their best hit in bacterial genomes from NCBI.

Sequence ID	Organisms of the best hit	Query Cover	E value	Identity	Accession
109SUR_14561	*Haliea salexigens* DSM 19537	100%	6E-134	100.0%	NZ_AUHJ01000005.1
18DCM_27808	*Hyphomonas atlantica*	100%	1E-123	87.5%	NZ_CP051254.1
18SUR_509	*Hyphomonas atlantica*	100%	1E-123	87.5%	NZ_CP051254.1
18SUR_3561	*Parvibaculum sedimenti*	99%	6E-96	72.0%	NZ_WESC01000013.1
18SUR_8583	*Haliea salexigens* DSM 19537	100%	6E-134	100.0%	NZ_AUHJ01000005.1
18SUR_21378	*Qipengyuania citrea* LAMA 915	100%	7E-127	95.2%	NZ_JYNE01000027.1
22SUR_924	*Hyphomonas atlantica*	100%	1E-123	87.5%	NZ_CP051254.1
22SUR_2298	*Haliea salexigens* DSM 19537	100%	6E-134	100.0%	NZ_AUHJ01000005.1
25DCM_8490	*Haliea alexandrii*	100%	1E-126	97.5%	NZ_RFLW01000002.1
25DCM_121821	*Hyphomonas atlantica*	100%	1E-123	87.5%	NZ_CP051254.1
25SUR_10745	*Hyphomonas atlantica*	100%	1E-123	87.5%	NZ_CP051254.1
31SUR_11329	*Aurantiacibacter xanthus*	100%	2E-117	84.4%	NZ_QXFM01000030.1
31SUR_20748	*Hyphomonas atlantica*	100%	1E-123	87.5%	NZ_CP051254.1
32DCM_38594	*Hyphomonas atlantica*	100%	5E-123	87.0%	NZ_CP051254.1
38DCM_5445	*Hyphomonas atlantica*	100%	1E-123	87.5%	NZ_CP051254.1
42SUR_77582	*Marinobacter adhaerens*	100%	6E-141	99.5%	NZ_CP076686.1
64SUR_4739	*Hyphomonas atlantica*	100%	1E-122	87.0%	NZ_CP051254.1
64SUR_4984	*Parvibaculum sedimenti*	100%	3E-118	84.9%	NZ_WESC01000013.1
64SUR_20581	*Marinobacter shengliensis*	100%	1E-139	100.0%	NZ_AP028062.1
65DCM_6713	*Qipengyuania citrea* LAMA 915	100%	7E-127	95.2%	NZ_JYNE01000027.1
66DCM_14035	*Hyphomonas*	100%	1E-123	87.5%	NZ_CP051254.1

	atlantica				
	Hyphomonas				
66SUR_3756	*atlantica*	100%	2E-125	90.9%	NZ_CP051254.1
	Hyphomonas				
66SUR_19196	*atlantica*	100%	5E-123	87.0%	NZ_CP051254.1
	Hyphomonas				
68SUR_4836	*atlantica*	100%	1E-123	87.5%	NZ_CP051254.1
	Haliea salexigens				
68SUR_36370	DSM 19537	100%	6E-134	100.0%	NZ_AUHJ01000005.1
	Hyphomonas				
70MES_12923	*atlantica*	100%	1E-123	87.5%	NZ_CP051254.1
	Hyphomonas				
72SUR_26968	*atlantica*	100%	1E-123	87.5%	NZ_CP051254.1
	Hyphomonas				
72SUR_79301	*atlantica*	100%	1E-134	99.0%	NZ_CP051254.1
	Marinobacter				
76DCM_29767	*salarius*	99%	3E-130	95.6%	NZ_CP020931.1
	Hyphomonas				
76DCM_31080	*atlantica*	100%	1E-123	87.5%	NZ_CP051254.1
	Qipengyuania				
76SUR_3176	*citrea* LAMA 915	100%	3E-125	94.7%	NZ_JYNE01000027.1
	Hyphomonas				
76SUR_9734	*atlantica*	100%	1E-123	87.5%	NZ_CP051254.1

Supplementary Table 6. Information on terrestrial metagenomes used in this study.

Metagenome	Accession Number	Biome	Location	Total number of sequences	Database
Rothamsted soil*	4453247.3	Temperate grasslands	Rothamsted, UK	1166789	MG-RAST
Forest soil*	4446153.3	Soil	Puerto Rico	689464	MG-RAST
Rice rhizosphere*	4449956.3	Soil	Los Banos, Philippines	1072868	MG-RAST
Maize soil	4935435.3	Cultivated environment	Urbana, Illinois, USA	101519133	MG-RAST

*, metagenomes analyzed by Carrión et al. (2015) for MddA homolgous.

Supplementary Table 7. General features of the *Halomonas* genomes.

Strains	Genome size (Mb)	Completeness (%)	G+C (%)	Number of CDS
Halomonas alimentaria EF61	5.29	99.57	63.7	4610
Halomonas alimentaria SCS19	4.90	99.57	64.0	4247
Halomonas alimentaria H10-9-1	3.79	100	66.1	3535
Halomonas saccharevitans H33-56	4.84	99.57	64.2	4223
Halomonas saccharevitans RT37	3.93	99.57	64.1	4339
Halomonas saccharevitans H10-59	4.78	99.57	64.2	4178

Supplementary Table 8. Plasmids used in this study.

Plasmids	Description and application
pBluescript SKII(-)	Clone vector used in constructing in-frame deletion mutant (Amp^R)
pK18mocsacB	Suicide plasmid used in constructing in-frame deletion mutant (Kan^R)
pRK2013	Assistant plasmid used in constructing in-frame deletion mutant (Kan^R)
pET24a (+)	*E. coli* T7 expression vector (Kan^R)
pUCm-T	Clone vector
pBBR1MCS-5	Clone vector used to complement the *mddH* mutation (Gmr)

Supplementary Table 9. Primers used in this study.

Primers	Sequence (5'-3')[a]	Product size (bp)	Function
mddH-UO	CG**GAATTC**AGGCATGATGCGCGACATGA	660	In-frame mutation
mddH-UI	TAGCCCGTCTCCATCCGCCCGTGTTGCCACACGCCAG		
mddH-DI	GCGGATGGAGACGGGCTATCTTTCG	766	In-frame mutation
mddH-DO	GC**TCTAGA**GCCTGAATCGCTGATGATGATGG		
mddHcom-F	CCC**AAGCTT**TCCCGGAGGAACGGGTGC	813	Complementation of in-frame mutation
mddHcom-R	CGC**GGATCC**TCAGCGGGGAACAGCAGC		
MddHPE-F	CCG**GAATTC**ATGTCCTTCTACGAGAATCGTGTTC	618	Heterologous expression of MddH
MddHPE-R	CCC**AAGCTT**GCGGGGAACAGCAGCC		
mddHrt-F	CCTACACCCTGTGCACGATT	285	RT-qPCR of *mddH*
mddHrt-R	CCCAGAAATTGAAGCCAGCG		
recArt-F	CCGGCAATATCAAGAACGCC	264	Reference gene for RT-qPCR
recArt-R	CCTTGCCGTAGAGGATCTGG		

[a] Nucleotides in bold represent restriction enzyme sites added to the 5′ region of the primers. Underlined nucleotides represent overlap sequences.

Supplementary Table 10. Functional and unfunctional MddH protein sequences in this study.

Strain	Protein sequence
Halomonas alimentaria EF61	MSFYENRVLPHFLHLACGNTVVDRQRAAVVPQARGRVLE VGMGSGLNIPHYDPDRVELVWGLEPSEGMRRKARHNVAS AQFEVRWLDLPGEEVPLDDNSVDTVVLTYTLCTIPDWHR ALEQMRRVLKPDGQLLFCEHGTAPDEAVRQWQRRINPLW RRVAGGCHLNRDIPELIGHAGFGIQRMETGYLSKAPRFAGF NFWGAAVPR
Algiphilus aromaticivorans DG1253	MAIYDHYVLPVVLDCCCGMKPIQKERAGLLPRARGRVLEI GIGTGRNFPFYAPEQVSSLIGLDPAEQMNAKARKRAAEAG MSVELMGVSAEGIPAEDNSFDTVVCTFSLCTIPDPVAALHE MRRVLKPEGELLFSEHGLAPEPKVQRWQHRLSPGWSKIA GGCQLDRDIPQLLDAGGFAIDEMREGYLKGPKPWTYVRT GWARAA
Marinobacter litoralis Sw-45	MSFYENRILPHIIDKACSMGQVMKLRSQVVPRAKGRVLEV GMGSGINLEFYDPDRVDMVYGLEPSEGMRRKAQVNLNRS SIKVEWLDLPGEKIPLEDHSVDTILLTFTLCTIPDWQAALK QMKRVLKPGGELLFLEHGESPDQGTCKWQHRITPGWKKL AGGCHLNRNIAELLKQGGFQIQELENLYIPKAPKIAGYIYK GVATNA
Pseudomonas pelagia CL-AP6	MSFYEDRILPHIIDKACSMGQVMKLRSQLVPRARGRVLEV GMGSGINLEFYNQDLVEMVYGLEPSEGMRRKALPNLGRS PVRVEWLDLPGEKIPLQDNSVDTVLLTFTLCTIPDWHTALL QMKRVLKPGGDLLFLEHGEAPHDTTRKWQHRITPGWRKL AGGCHLNRHIAELIEHAGFEIQELENLYMPNAPKIAGYIYK GRATKPE
Hyphomonas adhaerens MHS-3	MNPWEKYVVPNLISCACASKPMMKQREKVIPYAEGKVLE IGCGSGTNFSYYDPDKVEHLYALEPSGGMLKKARRAAGA LGYGNNIEFLETGAESVPLEDHSIDTVVYTFVLCTIPDWKG ALAETRRLLKPGGKIIFSEHGLAPDEGVAKWQRRVEPVWK PLAGGCHLTRDTNKMLEEAGFELQDAETMYLPGTPKIAG FCSWGSAVPV
Pyruvatibacter mobilis CGMCC_1.15125	MGFYEKHILPRFLDVACGAKPITYQRRKVVPQAEGRVLEI GMGSGLNLPYYDKAKVEMVFGLEPSEGMRERAAPRVKE AGIPVEFIDLPGEEIPLDANSVDTVLLTYTLCTIPDGIKALE GMARVLKPGGKLIFCEHGKAPDMGVARWQDRINPMWKK IAGGCNLNRPIPDMLAEGGFRIEGMEQMYLPSTPKFAGYN YWGQAVQG

Novosphingobium colocasiae KCTC 32255	MGLRHWWDDKVVPRLIRCACGHPSVMKVRSQVVPLAEG RVFEIGCGGGINQRFYDPARVTAYCGLDPSAKGLDFAREA ARVPDAQFVAGAGEQLPFPDDSFDTVVCTYTLCSVDDPGR TLAELRRVLKPGGALLYAEHGHAPDAGVARWQARIEPVW SSLAGNCHLTRPVTPAIAAAGFAPERMGAHYASGAPRFVS WMEWGRAVKPAV
Erythrobacter ramosus DSM 8510	MGITSWYEANVMPRLITCACSQGQVMKRRSAVVPLARGD VFELGCGGGINHAFYDPKAITSYAGIDPHEGLLDGARAAA RVKGWAADLRQGWGEAIPFDDASFDCVVCTFTLCSVSDP AQVMRELRRILRPGGQALFLEHGRAPDSDVRRWQQRIEP VWKRLAGGCHLTRPIAGALVGAGFAVETLGEGYTPKAPRF AGWMEWGIARKPQ
Ramlibacter aquaticus LMG 30558	MADNWYERHLLPTVLDFACGLPMVTRQRERVVPRARGR VLEVGIGTGLNMPHYAAEQVESITGVDPALRMHEKAKARI RRSGLKVELVGLSAERLPLADASFDTVLLTYTLCSIPEPVA ALREMRRVLAPGGRLLFCEHGRAPDASVRRWQARLQPW WGPIAGGCQLGRDIPALLVEAGFTLHGLETGYIPGPRPLAF NYWGEASA
Caulobacter henricii CB4	MTSFYDRHILPRVIGCACGAGAIAKQRAKIVPRAQGRVLE LGIGGGLNLAFYDPSRVSSVTGVDPSQGLR DRALAAPRPAGLNVEVLDGEAEQLSFESHSFDTVVCTFTL CSVHQPPAVLSEARRVLKPGGQFLFCEHGL APDAKVARWQKRLEPIWTPLAGGCRLTRPVGSGITAAGFV LDEIQAFYMPKAPRPLGWCELGVARAA
Vibrio sp. ZXX013 (UbiE homolog without Mdd activity)	MTDTSLQSNTALENETTHFGFSTVAKDEKVTKVAEVFHSV ATKYDIMNDLMSGGIHRLWKRFTIDCSGARPGQRILDLGG GTGDLTAKFSRIVGDEGHVILADINNSMLNVGRDKLRDNG IVGNVHYVQANAEELPFPDDYFDVITISFCLRNVTDKDKA LRSMFRVLKPGGRLLVLEFSKPVLEPLSKVYDAYSFHLLPR IGELVANDSESYRYLAESIRMHPDQETLEGMMQDAGFENT KYYNLTGGIVALHRGYKF

Reference

1. Choi, S. H. *et al.* Evidence for an Enzyme-Catalyzed Rauhut-Currier Reaction during the Biosynthesis of Spinosyn A. *J. Am. Chem. Soc.* **143**, 20291–20295 (2021).
2. Van Tran, N. *et al.* Evolutionary insights into Trm112-methyltransferase holoenzymes involved in translation between archaea and eukaryotes. *Nucleic Acids Res.* **46**, 8483–8499 (2018).
3. Cakici, O., Sikorski, M., Stepkowski, T., Bujacz, G. & Jaskolski, M. Crystal Structures of NodS N-Methyltransferase from Bradyrhizobium japonicum in Ligand-Free Form and as SAH Complex. *J. Mol. Biol.* **404**, 874–889 (2010).
4. Dai, Y. N. *et al.* Crystal structures and catalytic mechanism of the C-methyltransferase Coq5 provide insights into a key step of the yeast coenzyme Q synthesis pathway. *Acta Crystallogr. Sect. D Biol. Crystallogr.* **70**, 2085–2092 (2014).
5. Yu, F. *et al.* Crystal structure and enantioselectivity of terpene cyclization in SAM-dependent methyltransferase TleD. *Biochem. J.* **473**, 4385–4397 (2016).
6. Fenwick, M. K., Almabruk, K. H., Ealick, S. E., Begley, T. P. & Philmus, B. Biochemical Characterization and Structural Basis of Reactivity and Regioselectivity Differences between Burkholderia thailandensis and Burkholderia glumae 1,6-Didesmethyltoxoflavin N-Methyltransferase. *Biochemistry* **56**, 3934–3944 (2017).

The uncropped and unprocessed scans of supplementary Figure 3a.